

$B \rightarrow K^* \ell^+ \ell^-$ decays at large recoil in the Standard Model: a theoretical reappraisal

Marco Ciuchini^a, Marco Fedele^{b,c}, Enrico Franco^c, Satoshi Mishima^d, Ayan Paul^c,
Luca Silvestrini^c and Mauro Valli^{e,f}

^a*INFN, Sezione di Roma Tre, Via della Vasca Navale 84, I-00146 Roma, Italy*

^b*Dipartimento di Fisica, Università di Roma “La Sapienza”, P.le A. Moro 2, I-00185 Roma, Italy*

^c*INFN, Sezione di Roma, P.le A. Moro 2, I-00185 Roma, Italy*

^d*Theory Center, IPNS, KEK, Tsukuba 305-0801, Japan*

^e*SISSA, via Bonomea 265, I-34136 Trieste, Italy*

^f*INFN, Sezione di Trieste, via Valerio 2, I-34127 Trieste, Italy*

E-mail: marco.ciuchini@roma3.infn.it, enrico.franco@roma1.infn.it,
marco.fedele@uniroma1.it, satoshi.mishima@kek.jp,
ayan.paul@roma1.infn.it, luca.silvestrini@roma1.infn.it,
mauro.valli@sissa.it

ABSTRACT: We critically reassess the theoretical uncertainties in the Standard Model calculation of the $B \rightarrow K^* \ell^+ \ell^-$ observables, focusing on the low q^2 region. We point out that even optimized observables are affected by sizable uncertainties, since hadronic contributions generated by current-current operators with charm are difficult to estimate, especially for $q^2 \sim 4m_c^2 \simeq 6.8 \text{ GeV}^2$. We perform a detailed numerical analysis and present both predictions and results from the fit obtained using most recent data. We find that non-factorizable power corrections of the expected order of magnitude are sufficient to give a good description of current experimental data within the Standard Model. We discuss in detail the q^2 dependence of the corrections and their possible interpretation as shifts of the Standard Model Wilson coefficients.

Contents

1	Introduction	1
2	Power corrections to factorization at low q^2	2
3	Main results	5
4	Impact of improved measurements	13
5	Conclusions	13
A	Form factors	14
B	Helicity amplitudes in the Standard Model	16
C	Kinematic distribution	16
D	Angular observables	18
E	Tests and Cross-checks	21

1 Introduction

Flavour-Changing Neutral Current (FCNC) processes are very sensitive probes of New Physics (NP). Within the Standard Model (SM) they can only arise at the loop level, and they are further suppressed by the GIM cancellation mechanism, so that even very heavy new particles can give rise to sizable contributions, especially if they carry new sources of flavour violation. In particular, the semileptonic decays $B \rightarrow K^* \ell^+ \ell^-$ have been advocated to be among the cleanest FCNC processes [1–10]. Indeed, the dilepton invariant mass spectrum is accessible over the full kinematic range allowing to cut the theoretically challenging resonance-dominated regions. The description of the remaining part of the spectrum is simplified using the heavy quark expansion at low dilepton invariant mass q^2 [11, 12], while an Operator Product Expansion (OPE) can be used at large q^2 [13–16]. In particular, heavy quark symmetry allows to reduce the number of independent form factors [17–19], while non-factorizable corrections are power suppressed.¹ Experimentally, the full angular analysis can be performed allowing for the extraction of twelve angular coefficients (plus twelve more for the CP-conjugate decay) in several q^2 bins.² From these coefficients, exploiting the symmetries of the infinite mass limit, one can define “optimized” observables in which

¹This is not the case for charmonium resonant contributions. They need to be controlled using experimental cuts [20, 21].

²The number of independent angular coefficients reduces to eight neglecting the lepton masses.

the soft form factors cancel out, drastically reducing the theoretical uncertainties [22–24]. For these observables, very precise predictions can be found in the literature [25–39]. Some deviation from these predictions has been observed in recent LHCb data [40–43]. In this article we argue that no deviation is present once all the theoretical uncertainties are taken into account. Among those, the most important is a conservative evaluation of the deviation from the infinite mass limit. This kind of corrections is known to be important in other $b \rightarrow s$ decays [44–46]. In fact, nonperturbative contributions from non-leptonic operators with charm, although power suppressed, can compete with the contribution of semileptonic and radiative operators even below the $c\bar{c}$ threshold. A first estimate at small q^2 of this effect has been provided by ref. [47], showing indeed that these contributions are non-negligible. Furthermore, $c\bar{c}$ resonances at threshold give a contribution to the rate that is two orders of magnitude larger than the short-distance one [20, 21]; indeed, no OPE can be performed in this kinematical region, and quark-hadron duality is expected to hold only for $q^2 \ll 4m_c^2$. At present, the effect of power corrections and nonperturbative contributions cannot be fully computed from first principles. Unfortunately this is the main limiting factor in searching for NP in those amplitudes where these contributions are present. Indeed, underestimating them might lead to too early claims of NP. First steps towards a careful assessment of the hadronic uncertainties have been taken in refs. [48, 49].

In this work we show that, given the above arguments, present data do not unambiguously point to the presence of NP in $B \rightarrow K^*\ell^+\ell^-$. We will discuss below what kind of NP contributions can be disentangled from hadronic contributions; those which cannot be disentangled are hindered by the hadronic uncertainties.

This paper is organized as follows. In section 2 we discuss power corrections to factorized formulæ at low q^2 . In section 3 we present results and predictions, discussing the size and role of nonfactorizable terms. Our conclusions are drawn in section 5. Appendices A–E contain some technical details.

2 Power corrections to factorization at low q^2

Both $\bar{B} \rightarrow \bar{K}^*\ell^+\ell^-$ and $\bar{B} \rightarrow \bar{K}^*\gamma$ can be described by means of the $\Delta B = 1$ weak effective Hamiltonian

$$\mathcal{H}_{\text{eff}}^{\Delta B=1} = \mathcal{H}_{\text{eff}}^{\text{had}} + \mathcal{H}_{\text{eff}}^{\text{sl}+\gamma}, \quad (2.1)$$

where the first term is the hadronic contribution

$$\mathcal{H}_{\text{eff}}^{\text{had}} = \frac{4G_F}{\sqrt{2}} \left[\sum_{p=u,c} \lambda_p \left(C_1 Q_1^p + C_2 Q_2^p \right) - \lambda_t \left(\sum_{i=3}^6 C_i P_i + C_8 Q_{8g} \right) \right], \quad (2.2)$$

involving current-current, QCD penguin and chromomagnetic dipole operators [50]

$$\begin{aligned} Q_1^p &= (\bar{s}_L \gamma_\mu T^a p_L) (\bar{p}_L \gamma^\mu T^a b_L), \\ Q_2^p &= (\bar{s}_L \gamma_\mu p_L) (\bar{p}_L \gamma^\mu b_L), \\ P_3 &= (\bar{s}_L \gamma_\mu b_L) \sum_q (\bar{q} \gamma^\mu q), \\ P_4 &= (\bar{s}_L \gamma_\mu T^a b_L) \sum_q (\bar{q} \gamma^\mu T^a q), \end{aligned}$$

$$\begin{aligned}
P_5 &= (\bar{s}_L \gamma_{\mu 1} \gamma_{\mu 2} \gamma_{\mu 3} b_L) \sum_q (\bar{q} \gamma^{\mu 1} \gamma^{\mu 2} \gamma^{\mu 3} q), \\
P_6 &= (\bar{s}_L \gamma_{\mu 1} \gamma_{\mu 2} \gamma_{\mu 3} T^a b_L) \sum_q (\bar{q} \gamma^{\mu 1} \gamma^{\mu 2} \gamma^{\mu 3} T^a q), \\
Q_{8g} &= \frac{g_s}{16\pi^2} m_b \bar{s}_L \sigma_{\mu\nu} G^{\mu\nu} b_R,
\end{aligned} \tag{2.3}$$

while the second one, given by

$$\mathcal{H}_{\text{eff}}^{\text{sl}+\gamma} = -\frac{4G_F}{\sqrt{2}} \lambda_t \left(C_7 Q_{7\gamma} + C_9 Q_{9V} + C_{10} Q_{10A} \right), \tag{2.4}$$

includes the electromagnetic penguin plus the semileptonic operators

$$\begin{aligned}
Q_{7\gamma} &= \frac{e}{16\pi^2} m_b \bar{s}_L \sigma_{\mu\nu} F^{\mu\nu} b_R, \\
Q_{9V} &= \frac{\alpha_e}{4\pi} (\bar{s}_L \gamma_{\mu} b_L) (\bar{\ell} \gamma^{\mu} \ell), \\
Q_{10A} &= \frac{\alpha_e}{4\pi} (\bar{s}_L \gamma_{\mu} b_L) (\bar{\ell} \gamma^{\mu} \gamma^5 \ell),
\end{aligned} \tag{2.5}$$

where $\lambda_i \equiv V_{ib} V_{is}^*$ with $i = u, c, t$.

Considering the matrix element of $\mathcal{H}_{\text{eff}}^{\Delta B=1}$ in eq. (2.1) between the \bar{B} initial state and $\bar{K}^* \ell^+ \ell^-$ final state, the contribution of $\mathcal{H}_{\text{eff}}^{\text{sl}+\gamma}$ in eq. (2.4) clearly factorizes into the product of hadronic form factors and leptonic tensors at all orders in strong interactions. On the other hand, the matrix elements of $\mathcal{H}_{\text{eff}}^{\text{had}}$ in eq. (2.2) factorize only in the infinite m_b limit below the charm threshold [11, 12, 20]. Moreover, in this regime, heavy quark symmetry reduces the number of independent form factors from seven to two soft form factors [17–19]. Therefore, in this limit, the amplitudes have simpler expressions so that optimized observables dominated by short distance physics can be defined [22–24]. The main issue however is how important departures from the infinite mass limit are, in particular when q^2 is close to $4m_c^2$.

Concerning factorized amplitudes, these can be described using the full set of form factors, which have been estimated using QCD sum rules at low q^2 [9, 51–54]. In particular we use the very recent results of ref. [54] with the full correlation matrix. While the form factor calculation is a difficult one, we think that QCD sum rules provide a reasonable estimate of low q^2 values and uncertainties, compatible with the lattice estimate at high q^2 [55]. Using full QCD form factors reintroduces some hadronic uncertainties into optimized observables which have been estimated in refs. [25–30, 34, 35, 48, 49]. In this respect, it has been suggested in ref. [35] that including some power-suppressed terms in the definition of the soft functions could reduce the uncertainty on some optimized observables. Since observables cannot depend on arbitrary scheme definitions, their deviation from the infinite mass limit cannot be reduced in this way.

The main point of our paper concerns the non-factorizable contribution present in the matrix element of the Hamiltonian in equation (2.2) involving a $c\bar{c}$ loop. In the infinite mass limit, this term can be computed using QCD factorization including $\mathcal{O}(\alpha_s)$ corrections [12, 56]. Beyond the leading power, the contribution of $Q_{1,2}^c$ to the $\bar{B} \rightarrow \bar{K}^* \ell^+ \ell^-$ amplitude at $q^2 \sim 1 \text{ GeV}^2$, as well as the contribution to the $\bar{B} \rightarrow \bar{K}^* \gamma$ amplitude, has been estimated using light-cone sum rules in the single soft-gluon approximation [47]. This

approximation worsens as q^2 increases and breaks down at $q^2 \sim 4m_c^2$, as each additional soft gluon exchange is suppressed by a factor $1/(q^2 - 4m_c^2)$. In ref. [47] the authors proposed also a phenomenological model interpolating their result at $q^2 \sim 1 \text{ GeV}^2$ with a description of the resonant region based on dispersion relations. While this model is reasonable, clearly there are large uncertainties in the transition region from $q^2 \sim 4 \text{ GeV}^2$ to $m_{J/\psi}^2$. Therefore, we consider the result of ref. [47] at $q^2 \lesssim 1 \text{ GeV}^2$ as an estimate of the charm loop effect, but allow for larger effects as q^2 grows and reaches values of $\mathcal{O}(4m_c^2)$.

While $Q_{1,2}^c$ are expected to dominate the $\langle \bar{K}^* \gamma^* | \mathcal{H}_{\text{eff}}^{\text{had}} | \bar{B} \rangle$ matrix element, the effect of all operators in the hadronic Hamiltonian can be reabsorbed in the following parameterization, generalizing the one in ref. [48]:³

$$\begin{aligned} h_\lambda(q^2) &= \frac{\epsilon_\mu^*(\lambda)}{m_B^2} \int d^4x e^{iqx} \langle \bar{K}^* | T \{ j_{\text{em}}^\mu(x) \mathcal{H}_{\text{eff}}^{\text{had}}(0) \} | \bar{B} \rangle \\ &= h_\lambda^{(0)} + \frac{q^2}{1 \text{ GeV}^2} h_\lambda^{(1)} + \frac{q^4}{1 \text{ GeV}^4} h_\lambda^{(2)}, \end{aligned} \quad (2.6)$$

where $\lambda = +, -, 0$ represents the helicity. Notice that $h_\lambda^{(0)}$ and $h_\lambda^{(1)}$ could be reinterpreted as a modification of C_7 and C_9 respectively, while the term $h_\lambda^{(2)}$ that we introduce to allow for a growth of long-distance effects when approaching the charm threshold cannot be reabsorbed in a shift of the Wilson coefficients of the operators in eq. (2.1). We notice here the crucial point regarding NP searches in these processes: one cannot use data to disentangle long-distance contributions such as $h_\lambda^{(0,1)}$ from possible NP ones, except, of course, for NP-induced CP-violating effects and/or NP contributions to operators other than $C_{7,9}$. Thus, in the absence of a more accurate theoretical estimate of $h_\lambda(q^2)$ over the full kinematic range it is hardly possible to establish the presence of NP in $C_{7,9}$, unless its contribution is much larger than hadronic uncertainties. In this work we show that hadronic contributions are sufficient to reproduce the present data once all the uncertainties are properly taken into account. We conclude that, given the present hadronic uncertainties, the NP sensitivity of these decays is washed out. In order to recover it, a substantial reduction of these uncertainties is needed. This however requires a theoretical breakthrough in the calculation of the hadronic amplitude in eq. (2.6).

The $h_\lambda(q^2)$ are related to the $\tilde{g}^{\mathcal{M}_i}$ functions defined in ref. [47] as follows:

$$\begin{aligned} \tilde{g}^{\mathcal{M}_1} &= -\frac{1}{2C_1} \frac{16m_B^3(m_B + m_{K^*})\pi^2}{\sqrt{\lambda(q^2)}V(q^2)q^2} (h_-(q^2) - h_+(q^2)), \\ \tilde{g}^{\mathcal{M}_2} &= -\frac{1}{2C_1} \frac{16m_B^3\pi^2}{(m_B + m_{K^*})A_1(q^2)q^2} (h_-(q^2) + h_+(q^2)), \\ \tilde{g}^{\mathcal{M}_3} &= \frac{1}{2C_1} \left[\frac{64\pi^2 m_B^3 m_{K^*} \sqrt{q^2} (m_B + m_{K^*})}{\lambda(q^2) A_2(q^2) q^2} h_0(q^2) \right] \end{aligned} \quad (2.7)$$

³Since h_λ is a smooth function of q^2 in the range considered, the first hadronic threshold being at $q^2 = m_{J/\psi}^2 \sim 9.6 \text{ GeV}^2$, we are using a simple Taylor expansion. While the expansion might have significant corrections in the last bin considered, with current experimental uncertainties this is not problematic. We have also checked that using a parameterization with an explicit singularity at $m_{J/\psi}^2$ one obtains compatible results.

$$\left. -\frac{16m_B^3\pi^2(m_B+m_{K^*})(m_B^2-q^2-m_{K^*}^2)}{\lambda(q^2)A_2(q^2)q^2}(h_-(q^2)+h_+(q^2)) \right],$$

where the form factor definition is given in Appendix A. Notice that the nonfactorizable contribution to $\Delta C_9^i(q^2)$ is given by $2C_1\tilde{\gamma}^{\mathcal{M}_i}$. For the reader's convenience, we also give the expression of $\Delta C_7^i(0)$ in terms of $h_\lambda(0)$:

$$\begin{aligned}\Delta C_7^1(0) &= -\frac{8\pi^2 m_B^3}{\lambda^{1/2}(0)m_b T_1(0)}(h_-(0)-h_+(0)), \\ \Delta C_7^2(0) &= -\frac{8\pi^2 m_B^3}{\lambda^{1/2}(0)m_b T_1(0)}(h_-(0)+h_+(0)).\end{aligned}\tag{2.8}$$

In our analysis we let the complex parameters $h_\lambda^{(0,1,2)}$ vary in the range $|h_\lambda^{(0,1,2)}| < 2 \times 10^{-3}$ with arbitrary phase using flat priors. To comply with the expected power suppression of $h_+^{(0)}$ with respect to $h_-^{(0)}$, we impose that $|h_+^{(0)}/h_-^{(0)}| \leq 0.2$. We use the results in table 1 of ref. [47] at 1 GeV^2 as a constraint on $|h_\lambda|$ via eq. (2.7). We also use the results in eqs. (6.2)-(6.3) in the same paper at $q^2 = 0$ to further constrain $|h_\lambda|$ via eq. (2.8). As useful cross-checks, we also present in Appendix E the results of the analysis using as a constraint the phenomenological model of ref. [47] over the full q^2 range, obtaining results in agreement with the recent analysis of ref. [35], as well as the results of the analysis without using the constraints from ref. [47] at all.

3 Main results

We present the results for the Branching Ratios (BRs) and angular observables obtained performing a Bayesian analysis. We use the tool `HEPfit` [57] to compute all relevant observables and to estimate the p.d.f. performing a Markov Chain Monte Carlo (MCMC).⁴ The main input parameters are collected in table 1. They are the strong coupling, quark masses, meson decay constants, CKM parameters, the matching scale μ_W for the effective Hamiltonian, and the parameters λ_B and $a_{1,2}(\bar{K}^*)_{\perp,\parallel}$ describing properties of meson distribution functions entering the QCD factorization leading power expressions. The LHCb results from refs. [40, 42, 43, 59, 60] are reported in tables 2 and 3 for the reader's convenience (we do not report here the correlation matrices for LHCb results, which are used in our analysis).⁵ We use the form factors from [54] (details can be found in Appendix A). All Wilson coefficients are computed at NNLO at 4.8 GeV [61–64].

In figure 1 we present the results for the $B \rightarrow K^*\mu^+\mu^-$ angular observables of the full fit to all the LHCb measurements reported in tables 2 and 3. The corresponding numerical results are reported in the “full fit” column of table 2, while in table 3 we report the numerical results for the $B \rightarrow K^*e^+e^-$ observables.

Let us now discuss the compatibility of the SM with experimental data, taking theoretical and experimental correlations into account. For uncorrelated observables, such as

⁴`HEPfit` uses a parallelized version of the Bayesian Analysis Toolkit (BAT) library [58] to perform MCMC runs.

⁵In ref. [43] the data are analysed using three different methods. We use the unbinned maximum likelihood fit, which is the most accurate one.

Parameters	Mean Value	Uncertainty	Reference
$\alpha_s(M_Z)$	0.1185	0.0005	[65]
m_t (GeV)	173.34	0.76	[66]
$m_c(m_c)$ (GeV)	1.28	0.02	[67]
$m_b(m_b)$ (GeV)	4.17	0.05	[68]
f_{B_s} (MeV)	226	5	[69]
f_{B_s}/f_{B_d}	1.204	0.016	[69]
$f_{K^*,\parallel}$ (MeV)	225	30	[70]
$f_{K^*,\perp}(1\text{GeV})$ (MeV)	185	10	[70]
λ	0.2250	0.0006	[71, 72]
A	0.829	0.012	[71, 72]
$\bar{\rho}$	0.132	0.018	[71, 72]
$\bar{\eta}$	0.348	0.012	[71, 72]
μ_W (GeV)	100	60	
λ_B (MeV)	350	150	[56]
$a_1(\bar{K}^*)_{\perp,\parallel}$	0.2	0.1	[12, 70]
$a_2(\bar{K}^*)_{\perp,\parallel}$	0.05	0.1	[12, 70]

Table 1. Parameters varied in the analysis. The last four parameters have flat priors with half width reported in the third column. The remaining ones have Gaussian prior. Meson masses, lepton masses, s -quark mass and electroweak couplings are fixed at the PDG value [65].

BR's and $B \rightarrow K^* e^+ e^-$ angular observables, one can simply remove the experimental information on a particular observable from the fit to obtain a “prediction” for that observable, and then compute the p -value (see table 2 and 3). In the case of correlated observables, one can generalize this procedure to take all correlations into account. Since the angular observables in each bin are correlated, we proceed as follows: we remove the experimental information in one bin at a time from the fit to obtain the “predictions” reported in the corresponding column in table 2, as well as their correlation matrix. Adding the experimental covariance matrix to the one obtained from the fit, we compute the log likelihood and report in table 2 the corresponding p -value. For completeness, we also give in table 2 our results and predictions for the $B \rightarrow K^* \mu^+ \mu^-$ optimized observable P'_5 , which is however not independent from the other observables in table 2.⁶

The results for the parameters defining the nonfactorizable power corrections h_λ are reported in table 4 (in this case, the distributions are not Gaussian). It is interesting to notice that $|h_-^{(2)}|$ is different from zero at more than 95.45% probability (see figure 2), thus disfavouring the interpretation of the hadronic correction as a modified Wilson coefficient for operators $Q_{7,9}$, possibly generated by NP contributions.

For an easy comparison with ref. [47], we also report in figure 3 the results of the fit for the absolute value of the \tilde{g}_i functions, together with the phenomenological model proposed in the same work. The sizable q^2 dependence of hadronic corrections is visible by eye in

⁶In this case, we quote a “naive” p -value obtained neglecting the correlation with other observables.

this plot.

The reader may wonder how the results presented so far depend on our assumptions on the size and shape of nonfactorizable power corrections. To elucidate this interesting point, we performed a number of tests and cross-checks. Let us summarize our findings here and relegate detailed numerical results to Appendix E. If we do not use the numerical information from ref. [47], we obtain (as expected) an even better fit of experimental data (see tables 7 and 10, and figure 5) with a completely reasonable posterior for the power corrections, reported in table 5 and in figure 4. It is evident that the SM calculation supplemented with purely data-driven nonfactorizable power corrections of the expected order of magnitude is fully compatible with the data. In this case, however, the determination from data of the \tilde{g}_i functions is less precise, and no firm conclusion can be drawn on the size of the $h_\lambda^{(2)}$ term.

Finally, for the sake of comparison, we also present in Appendix E the results obtained adopting the phenomenological model of ref. [47] for the q^2 dependence of the power corrections, although we consider this model to be inadequate for $q^2 \sim 4m_c^2$ as discussed in section 2. In this case, we reproduce the results in the literature, with large deviations in several angular observables (see tables 8 and 11, and figure 6). For completeness, we also report in the same Appendix the results of a fit assuming vanishing $h_\lambda^{(2)}$, i.e. hadronic corrections fully equivalent to a shift in $C_{7,9}$ (tables 9 and 12, and figure 7).

We close this section by comparing the above scenarios using the Information Criterion [76, 77], defined as

$$IC = -2\overline{\log L} + 4\sigma_{\log L}^2, \quad (3.1)$$

where $\overline{\log L}$ is the average of the log-likelihood and $\sigma_{\log L}^2$ is its variance. Preferred models are expected to give smaller IC values. If we ignore the constraints from the calculation in ref. [47], we obtain $IC \sim 72$; using the calculation of ref. [47] at $q^2 \leq 1 \text{ GeV}^2$ yields $IC \sim 78$; doing the same but dropping the $h_\lambda^{(2)}$ terms gives $IC \sim 81$, while using the model of ref. [47] over the full q^2 range yields $IC \sim 111$. This confirms that the phenomenological model proposed in ref. [47] does not give a satisfactory description of experimental data, while the Standard Model supplemented with the hadronic corrections in eq. (2.6) provides a much better fit, even when the results of ref. [47] at $q^2 \leq 1 \text{ GeV}^2$ are used. In this case, a nonvanishing q^4 term is preferred.

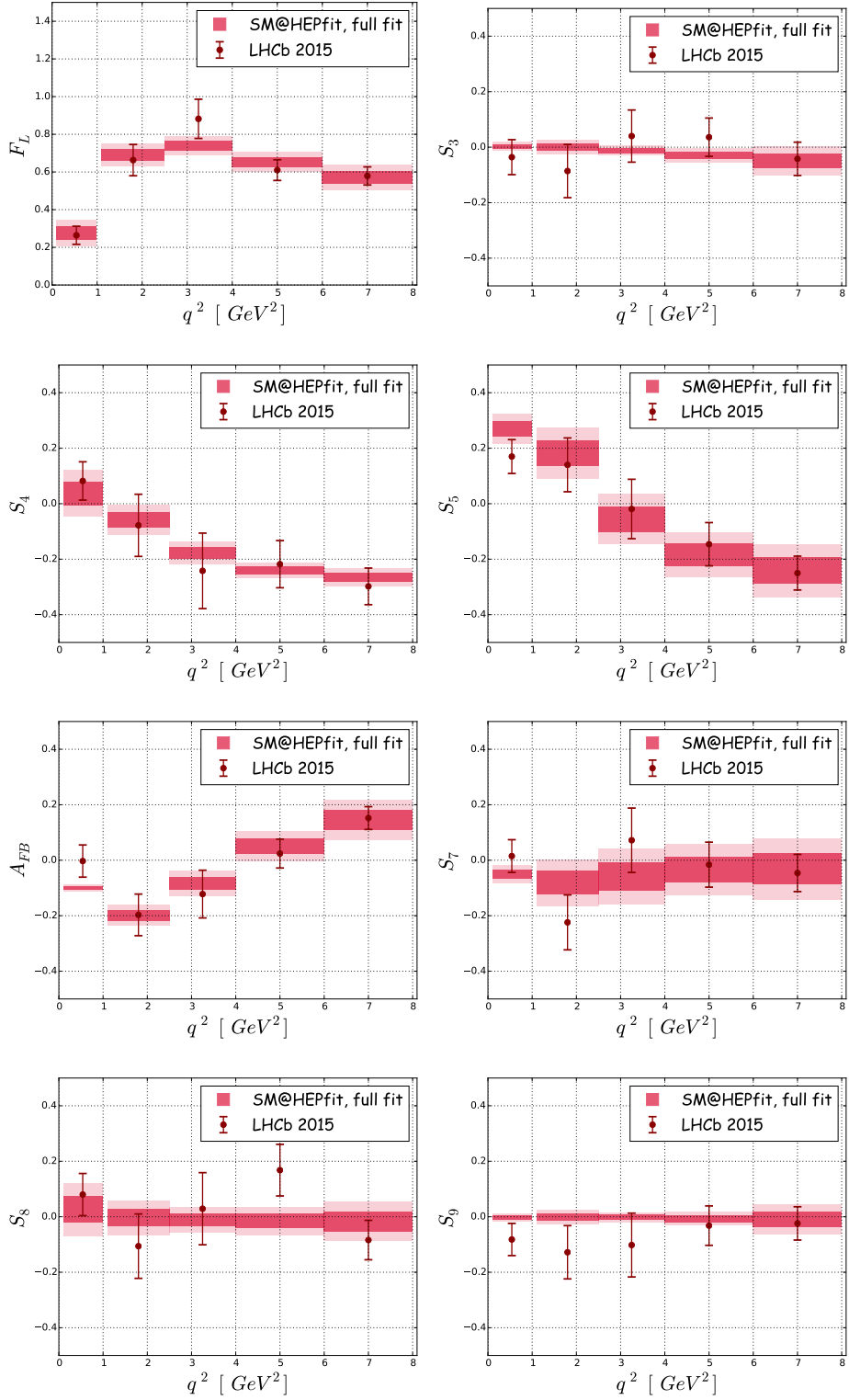


Figure 1. Results of the full fit and experimental results for the $B \rightarrow K^* \mu^+ \mu^-$ angular observables. Here and in the following, we use darker (lighter) colours for the 68% (95%) probability regions.

q^2 bin [GeV ²]	Observable	measurement	full fit	prediction	p – value
[0.1, 0.98]	F_L	0.264 ± 0.048	0.275 ± 0.035	0.257 ± 0.035	0.13
	S_3	-0.036 ± 0.063	0.002 ± 0.008	0.002 ± 0.008	
	S_4	0.082 ± 0.069	0.037 ± 0.042	-0.025 ± 0.047	
	S_5	0.170 ± 0.061	0.271 ± 0.027	0.301 ± 0.024	
	A_{FB}	-0.003 ± 0.058	-0.102 ± 0.006	-0.104 ± 0.006	
	S_7	0.015 ± 0.059	-0.049 ± 0.016	-0.043 ± 0.017	
	S_8	0.080 ± 0.076	0.027 ± 0.048	-0.004 ± 0.046	
	S_9	-0.082 ± 0.058	-0.002 ± 0.007	-0.002 ± 0.007	
	P'_5	0.387 ± 0.142	0.774 ± 0.094	0.881 ± 0.082	
	[1.1, 2.5]	F_L	0.663 ± 0.083	0.691 ± 0.030	0.688 ± 0.034
S_3		-0.086 ± 0.096	0.000 ± 0.013	0.001 ± 0.013	
S_4		-0.078 ± 0.112	-0.059 ± 0.027	-0.070 ± 0.032	
S_5		0.140 ± 0.097	0.183 ± 0.046	0.208 ± 0.057	
A_{FB}		-0.197 ± 0.075	-0.198 ± 0.019	-0.200 ± 0.022	
S_7		-0.224 ± 0.099	-0.081 ± 0.042	-0.056 ± 0.049	
S_8		-0.106 ± 0.116	-0.003 ± 0.031	-0.004 ± 0.033	
S_9		-0.128 ± 0.096	-0.002 ± 0.013	0.002 ± 0.013	
P'_5		0.298 ± 0.212	0.410 ± 0.099	0.460 ± 0.120	0.51
[2.5, 4]		F_L	0.882 ± 0.104	0.739 ± 0.025	0.729 ± 0.028
	S_3	0.040 ± 0.094	-0.012 ± 0.009	-0.014 ± 0.010	
	S_4	-0.242 ± 0.136	-0.176 ± 0.020	-0.179 ± 0.021	
	S_5	-0.019 ± 0.107	-0.055 ± 0.045	-0.055 ± 0.052	
	A_{FB}	-0.122 ± 0.086	-0.082 ± 0.023	-0.082 ± 0.025	
	S_7	0.072 ± 0.116	-0.059 ± 0.050	-0.080 ± 0.055	
	S_8	0.029 ± 0.130	-0.012 ± 0.023	-0.012 ± 0.023	
	S_9	-0.102 ± 0.115	-0.003 ± 0.009	-0.003 ± 0.009	
	P'_5	-0.077 ± 0.354	-0.130 ± 0.100	-0.130 ± 0.120	0.89
	[4, 6]	F_L	0.610 ± 0.055	0.653 ± 0.026	0.661 ± 0.030
S_3		0.036 ± 0.069	-0.030 ± 0.013	-0.030 ± 0.015	
S_4		-0.218 ± 0.085	-0.241 ± 0.014	-0.239 ± 0.016	
S_5		-0.146 ± 0.078	-0.183 ± 0.040	-0.205 ± 0.046	
A_{FB}		0.024 ± 0.052	0.050 ± 0.027	0.067 ± 0.032	
S_7		-0.016 ± 0.081	-0.034 ± 0.046	-0.037 ± 0.055	
S_8		0.168 ± 0.093	-0.015 ± 0.025	-0.026 ± 0.026	
S_9		-0.032 ± 0.071	-0.007 ± 0.012	-0.012 ± 0.014	
P'_5		-0.301 ± 0.160	-0.388 ± 0.087	-0.440 ± 0.100	0.46
[6, 8]		F_L	0.579 ± 0.048	0.569 ± 0.034	0.517 ± 0.070
	S_3	-0.042 ± 0.060	-0.050 ± 0.026	-0.006 ± 0.054	
	S_4	-0.298 ± 0.066	-0.264 ± 0.016	-0.224 ± 0.037	
	S_5	-0.250 ± 0.061	-0.241 ± 0.048	-0.164 ± 0.100	
	A_{FB}	0.152 ± 0.041	0.146 ± 0.036	0.099 ± 0.077	
	S_7	-0.046 ± 0.067	-0.031 ± 0.055	0.010 ± 0.110	
	S_8	-0.084 ± 0.071	-0.017 ± 0.035	0.039 ± 0.055	
	S_9	-0.024 ± 0.060	-0.011 ± 0.027	0.018 ± 0.047	
	P'_5	-0.505 ± 0.124	-0.491 ± 0.098	-0.330 ± 0.200	0.46
	[0.1, 2]	BR $\cdot 10^7$	0.58 ± 0.09	0.65 ± 0.04	0.67 ± 0.04
[2, 4.3]	0.29 ± 0.05		0.33 ± 0.03	0.35 ± 0.04	0.35
[4.3, 8.68]	0.47 ± 0.07		0.45 ± 0.05	0.47 ± 0.11	1.0
	BR $_{B \rightarrow K^* \gamma} \cdot 10^5$	4.33 ± 0.15	4.35 ± 0.14	4.61 ± 0.56	0.63

Table 2. Experimental results (with symmetrized errors), results from the full fit, predictions and p-values for $B \rightarrow K^* \mu^+ \mu^-$ BR's and angular observables. The predictions are obtained removing the corresponding observable from the fit. For the angular observables, since their measurements are correlated in each bin, we remove from the fit the experimental information on all angular observables in one bin at a time to obtain the predictions. See the text for details. We also report the results for $BR(B \rightarrow K^* \gamma)$ (including the experimental value from refs. [65, 73–75]) and for the optimized observable P'_5 . The latter is however not explicitly used in the fit as a constraint, since it is not independent of F_L and S_5 .

Observable	measurement	full fit	prediction	p-value
P_1	-0.23 ± 0.24	0.00 ± 0.01	0.00 ± 0.01	0.34
P_2	0.05 ± 0.09	-0.040 ± 0.00	-0.040 ± 0.00	0.32
P_3	-0.07 ± 0.11	0.00 ± 0.01	0.00 ± 0.01	0.53
F_L	0.16 ± 0.08	0.170 ± 0.04	0.18 ± 0.05	0.82
$\text{BR} \cdot 10^7$	3.1 ± 1.0	1.4 ± 0.1	1.4 ± 0.1	0.06

Table 3. *Experimental results (with symmetrized errors), results from the full fit, predictions and p-values for $B \rightarrow K^* e^+ e^-$ BR and angular observables. The predictions are obtained removing the corresponding observable from the fit.*

Parameter	Absolute value	Phase (rad)
$h_0^{(0)}$	$(5.7 \pm 2.0) \cdot 10^{-4}$	3.57 ± 0.55
$h_0^{(1)}$	$(2.3 \pm 1.6) \cdot 10^{-4}$	0.1 ± 1.1
$h_0^{(2)}$	$(2.8 \pm 2.1) \cdot 10^{-5}$	-0.2 ± 1.7
$h_+^{(0)}$	$(7.9 \pm 6.9) \cdot 10^{-6}$	0.1 ± 1.7
$h_+^{(1)}$	$(3.8 \pm 2.8) \cdot 10^{-5}$	-0.7 ± 1.9
$h_+^{(2)}$	$(1.4 \pm 1.0) \cdot 10^{-5}$	3.5 ± 1.6
$h_-^{(0)}$	$(5.4 \pm 2.2) \cdot 10^{-5}$	3.2 ± 1.4
$h_-^{(1)}$	$(5.2 \pm 3.8) \cdot 10^{-5}$	0.0 ± 1.7
$h_-^{(2)}$	$(2.5 \pm 1.0) \cdot 10^{-5}$	0.09 ± 0.77

Table 4. *Results for the parameters defining the nonfactorizable power corrections h_λ obtained using the numerical information from ref. [47] for $q^2 \leq 1 \text{ GeV}^2$.*

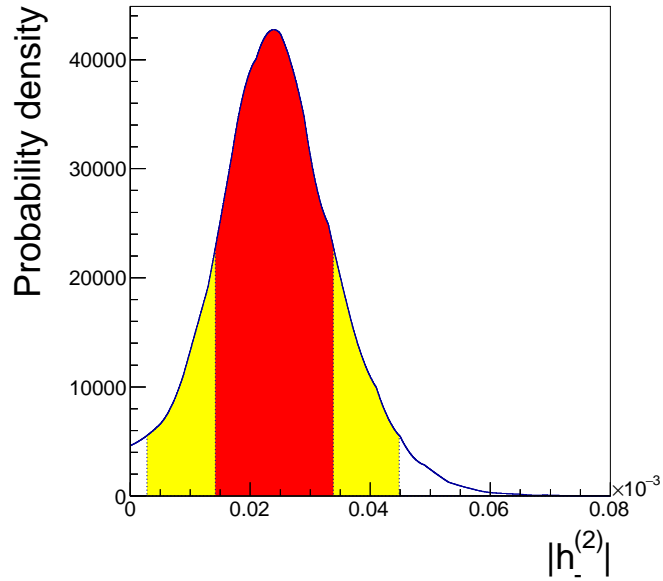


Figure 2. *P.d.f. for the hadronic parameter $|h_-^{(2)}|$ obtained using the numerical information from ref. [47] for $q^2 \leq 1 \text{ GeV}^2$.*

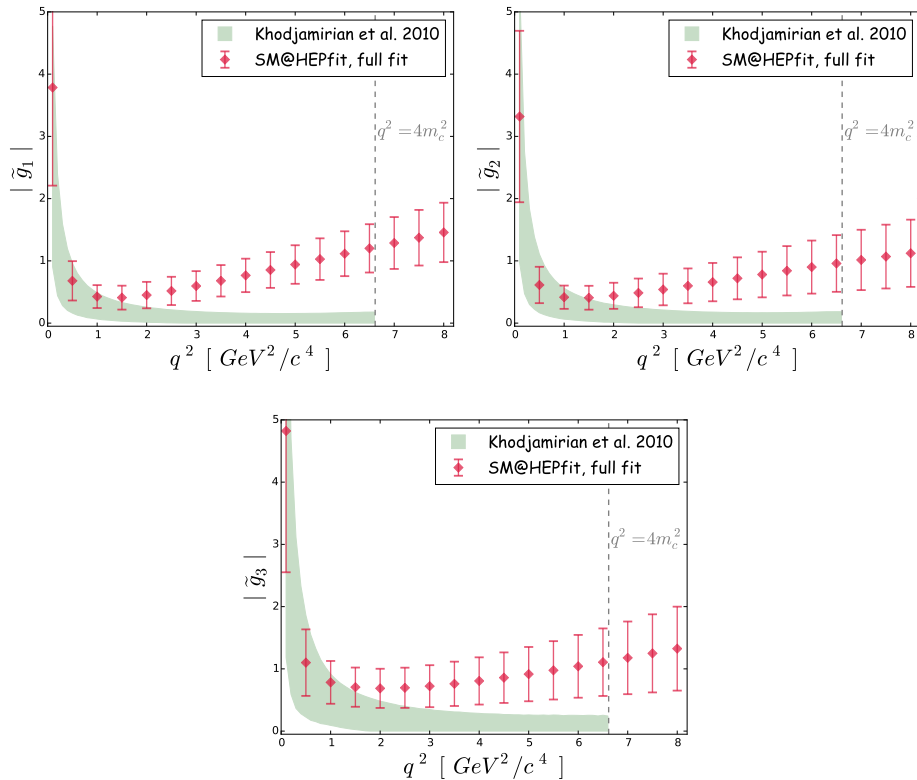


Figure 3. *Results of the fit for $|\tilde{g}_{1,2,3}|$ defined in ref. [47] as a function of q^2 together with the phenomenological parametrization suggested in the same paper.*

Parameter	Absolute value	Phase (rad)
$h_0^{(0)}$	$(5.8 \pm 2.1) \cdot 10^{-4}$	3.54 ± 0.56
$h_0^{(1)}$	$(2.9 \pm 2.1) \cdot 10^{-4}$	0.2 ± 1.1
$h_0^{(2)}$	$(3.4 \pm 2.8) \cdot 10^{-5}$	-0.4 ± 1.7
$h_+^{(0)}$	$(4.0 \pm 4.0) \cdot 10^{-5}$	0.2 ± 1.5
$h_+^{(1)}$	$(1.4 \pm 1.1) \cdot 10^{-4}$	0.1 ± 1.7
$h_+^{(2)}$	$(2.6 \pm 2.0) \cdot 10^{-5}$	3.8 ± 1.3
$h_-^{(0)}$	$(2.5 \pm 1.5) \cdot 10^{-4}$	$1.85 \pm 0.45 \cup 4.75 \pm 0.75$
$h_-^{(1)}$	$(1.2 \pm 0.9) \cdot 10^{-4}$	$-0.90 \pm 0.70 \cup 0.80 \pm 0.80$
$h_-^{(2)}$	$(2.2 \pm 1.4) \cdot 10^{-5}$	0.0 ± 1.2

Table 5. Results for the parameters defining the nonfactorizable power corrections h_λ obtained without using the numerical information from ref. [47].

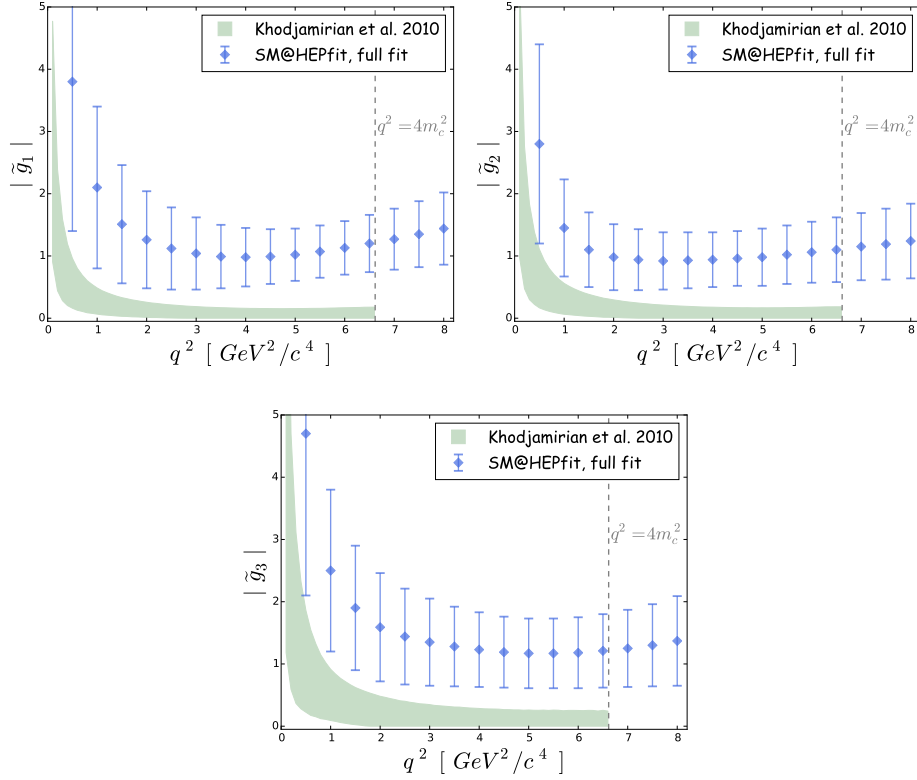


Figure 4. Same plots as in figure 3 obtained without using the results of ref. [47] for $q^2 \leq 1 \text{ GeV}^2$ in the fit.

4 Impact of improved measurements

In this section, we study how our determination of $h_\lambda(q^2)$ would improve if all experimental errors in Table 2 were improved by an order of magnitude, keeping fixed the central values of the hadronic parameters.

	using ref. [47] at $q^2 < 1 \text{ GeV}^2$		not using ref. [47]	
Parameter	$\frac{\delta \text{ abs}}{\text{abs}}$	$\delta \text{ arg (rad)}$	$\frac{\delta \text{ abs}}{\text{abs}}$	$\delta \text{ arg (rad)}$
$h_0^{(0)}$	$\pm 10\%$	± 0.07	$\pm 10\%$	± 0.09
$h_0^{(1)}$	$\pm 20\%$	± 0.2	$\pm 20\%$	± 0.3
$h_0^{(2)}$	$\pm 30\%$	± 0.3	$\pm 30\%$	± 0.4
$h_+^{(0)}$	$\pm 80\%$	± 1.4	$\pm 90\%$	± 1.4
$h_+^{(1)}$	$\pm 70\%$	± 1.6	$\pm 60\%$	± 1.4
$h_+^{(2)}$	$\pm 30\%$	± 0.4	$\pm 30\%$	± 0.3
$h_-^{(0)}$	$\pm 40\%$	± 0.8	$\pm 50\%$	± 1.0
$h_-^{(1)}$	$\pm 30\%$	± 0.5	$\pm 30\%$	± 0.5
$h_-^{(2)}$	$\pm 14\%$	± 0.1	$\pm 14\%$	± 0.2

Table 6. Results for the parameters defining the nonfactorizable power corrections h_λ obtained using experimental errors reduced by one order of magnitude.

We show the results for the coefficients $h_\lambda^{(0,1,2)}$ in Table 6. There is a significant reduction of the uncertainty on the coefficients $h_0^{(0,1,2)}$ and on $h_\pm^{(2)}$. Furthermore, the dependence of the fit on the theoretical estimate of ref. [47] is removed to a large extent. This exercise shows that future measurements, depending of course on their central values, could allow for an unambiguous determination of the q^4 terms in h_λ , even without theoretical input.

5 Conclusions

In this work, we critically examined the theoretical uncertainty in the SM analysis of $B \rightarrow K^* \ell^+ \ell^-$ decays, with particular emphasis on the nonfactorizable corrections in the region of $q^2 \lesssim 4m_c^2$. Using all available theoretical information within its domain of validity we performed a fit to the experimental data and found no significant discrepancy with the SM. This requires the presence of sizable, yet perfectly acceptable, nonfactorizable power corrections. Assuming the validity of the QCD sum rules estimate of these power corrections at $q^2 \leq 1 \text{ GeV}^2$, we observe a q^2 dependence of the nonfactorizable contributions (in particular a nonvanishing $h_-^{(2)}$), which disfavours their interpretation as a shift of the SM Wilson coefficients at more than 95.45% probability. A fit performed without using any theoretical estimate of the nonfactorizable corrections yields a range for these contributions larger than, but in the same ballpark of, the QCD sum rule calculation. In this case, unfortunately, no conclusion on the presence of q^4 terms in h_λ can be drawn. We conclude

that no evidence of CP-conserving NP contributions to the Wilson coefficients $C_{7,9}$ can be inferred from these decays unless a theoretical breakthrough allows us to obtain an accurate estimate of nonfactorizable power corrections and to disentangle possible NP contributions from hadronic uncertainties. Nevertheless, an improved set of measurements could possibly clarify the issue of the q^2 dependence of h_λ .

Of course, there might be other measurements, such as R_K [78], hinting at possible NP contributions which may well play a role also in $B \rightarrow K^* \ell^+ \ell^-$. In this case, a global fit could benefit also from the information provided by $B \rightarrow K^* \ell^+ \ell^-$ decays [32, 33, 36–39, 49, 54, 79].

Acknowledgments

The research leading to these results has received funding from the European Research Council under the European Union’s Seventh Framework Programme (FP/2007-2013) / ERC Grant Agreements n. 279972 “NPFlavour” and n. 267985 “DaMeSyFla”. M.C. is associated to the Dipartimento di Matematica e Fisica, Università di Roma Tre, and E.F. and L.S. are associated to the Dipartimento di Fisica, Università di Roma “La Sapienza”. We thank J. Matias for pointing out a numerical error in our evaluation of S_4 in the first version of this manuscript. It is a pleasure to thank T. Blake, C. Bobeth, J. Camalich, G. D’Agostini, S. Jäger, A. Khodjamirian, N. Serra, V. Vagnoni, J. Virto, M. Wingate, and R. Zwicky for interesting discussions.

A Form factors

There have been some recent developments in the computation of the form factor in both the large and small recoil regions. In the low q^2 regime the form factors derived using LCSR [52, 53] have been recomputed with more precise hadronic inputs for $q^2 = 0$. The extrapolation of the form factors into the finite q^2 region below 10 GeV² is now done with a new parametrization [54], as opposed to the old one found in [52]. This parametrization is akin to what has been used by the lattice group [55, 80] for their computations of the form factors in the high q^2 region and is adopted to follow the explicit symmetry relations that need to be imposed on the form factors at the lower kinematic endpoint. The other new development is that the parametrization now comes with a full correlation matrix that we use in our fits. In this section we shall briefly outline these developments so as to make the presentation comprehensive.

In the helicity basis the seven $B \rightarrow V$ form factors, with V being a vector meson, can be written in terms of those in the transversality basis

$$\begin{aligned} V_0(q^2) &= \frac{1}{2m_V \lambda^{1/2} (m_B + m_V)} [(m_B + m_V)^2 (m_B^2 - q^2 - m_V^2) A_1(q^2) - \lambda A_2(q^2)], \\ V_\pm(q^2) &= \frac{1}{2} \left[\left(1 + \frac{m_V}{m_B}\right) A_1(q^2) \mp \frac{\lambda^{1/2}}{m_B (m_B + m_V)} V(q^2) \right], \\ T_0(q^2) &= \frac{m_B}{2m_V \lambda^{1/2}} \left[(m_B^2 + 3m_V^2 - q^2) T_2(q^2) - \frac{\lambda}{m_B^2 - m_V^2} T_3(q^2) \right], \end{aligned}$$

$$\begin{aligned}
T_{\pm}(q^2) &= \frac{m_B^2 - m_V^2}{2m_B^2} T_2(q^2) \mp \frac{\lambda^{1/2}}{2m_B^2} T_1(q^2), \\
S(q^2) &= A_0(q^2).
\end{aligned} \tag{A.1}$$

Adopting the notation of [80] one can redefine

$$\begin{aligned}
A_{12}(q^2) &= \frac{(m_B + m_V)^2 (m_B^2 - m_V^2 - q^2) A_1(q^2) - \lambda(q^2) A_2(q^2)}{16m_B m_V^2 (m_B + m_V)}, \\
T_{23}(q^2) &= \frac{(m_B^2 - m_V^2) (m_B^2 + 3m_V^2 - q^2) T_2(q^2) - \lambda(q^2) T_3(q^2)}{8m_B m_V^2 (m_B - m_V)}.
\end{aligned} \tag{A.2}$$

The form factors \tilde{V}^0 and \tilde{T}^0 that appear in the helicity amplitudes are defined as

$$\tilde{V}^0(q^2) = \frac{4m_V}{\sqrt{q^2}} A_{12}(q^2) \quad \text{and} \quad \tilde{T}^0(q^2) = \frac{2\sqrt{q^2} m_V}{m_B(m_B + m_V)} T_{23}(q^2). \tag{A.3}$$

The rest of the helicity form factors are defined as

$$\begin{aligned}
\tilde{V}_{L\pm}(q^2) &= -\tilde{V}_{R\mp}(q^2) = V_{\pm}(q^2), \\
\tilde{T}_{L\pm}(q^2) &= -\tilde{T}_{R\mp}(q^2) = T_{\pm}(q^2), \\
\tilde{S}_L(q^2) &= -\tilde{S}_R(q^2) = S(q^2).
\end{aligned} \tag{A.4}$$

There are some symmetry relations between the form factors at $q^2 = 0$. These relations are used in deriving the parametric fits in [54] resulting in a correlation between the different form factors which we use in our computation of the observables. These can be written as

$$A_{12}(0) = \frac{m_B^2 - m_{K^*}^2}{8m_B m_{K^*}} A_0(0) \quad \text{and} \quad T_1(0) = T_2(0). \tag{A.5}$$

The form factors can now be parametrized in terms of $z(t)$ defined as

$$z(t) = \frac{\sqrt{t_+ - t} - \sqrt{t_+ - t_0}}{\sqrt{t_+ - t} + \sqrt{t_+ - t_0}}, \tag{A.6}$$

with

$$t_{\pm} = (m_B \pm m_V)^2, \quad t_0 = t_+(1 - \sqrt{1 - t_-/t_+}) \quad \text{and} \quad t = q^2. \tag{A.7}$$

The fit function used in [54] fits the form factors with the expansion

$$F_i(q^2) = P_i(q^2) \sum_k \alpha_k^i [z(q^2) - z(0)]^k, \tag{A.8}$$

where $P_i(q^2) = (1 - q^2/m_{R,i}^2)^{-1}$. The central values of the parameters α_k^i along with the errors and correlations can be found in the ancillary files in the arXiv entry of [54].⁷ The values of $m_{R,i}$ corresponding to the first resonance in the spectrum can be found in table 3 of [54].

⁷We use the fit based on LCSR results only.

B Helicity amplitudes in the Standard Model

Since our analysis primarily focuses on the SM, we shall present here the helicity amplitudes that are relevant for this analysis. The entire list of helicity amplitudes including the chirality flipped contributions can be found in [48] from where we derive our notation. The most significant amongst the helicity amplitudes are the vector and axial ones. The pseudoscalar one gets contributions from SM but is suppressed by the mass of the lepton and hence is numerically significant only in the lowest q^2 bin. The scalar helicity amplitude does not get any contribution from the SM. The tensor helicity amplitudes will not be considered here since they are missing in the literature and addressing that is out of the scope of this work. However, their expected contribution to the observables is not significant [48]. Stripping the relevant helicity amplitudes to the bare minimum relevant for our SM computation we have:⁸

$$\begin{aligned} H_V^\lambda &= -iN \left\{ C_9^{\text{eff}} \tilde{V}_{L\lambda} + \frac{m_B^2}{q^2} \left[\frac{2m_b}{m_B} C_7^{\text{eff}} \tilde{T}_{L\lambda} - 16\pi^2 h_\lambda \right] \right\}, \\ H_A^\lambda &= -iN C_{10} \tilde{V}_{L\lambda}, \\ H_P &= iN \frac{2m_l m_b}{q^2} C_{10} \left(\tilde{S}_L - \frac{m_s}{m_B} \tilde{S}_R \right), \end{aligned} \quad (\text{B.1})$$

where

$$N = -\frac{4G_F m_B}{\sqrt{2}} \frac{e^2}{16\pi^2} \lambda_t \quad (\text{B.2})$$

is a normalisation factor, and h_λ contains all the non-factorizable hadronic contributions, as discussed in section 2.

Observing now that the radiative decay $B \rightarrow V\gamma$ is described by a subset of the helicity amplitudes involved in the $B \rightarrow V\ell^+\ell^-$ decay, following [48] it is possible to write

$$A(\bar{B} \rightarrow V(\lambda)\gamma(\lambda)) = \frac{iN m_B^2}{e} \left[\frac{2m_b}{m_B} C_7 \tilde{T}_\lambda(q^2=0) - 16\pi^2 h_\lambda(q^2=0) \right]. \quad (\text{B.3})$$

The definitions and values of all the parameters used in this analysis are given in table 1.

C Kinematic distribution

Considering the full decay of the K^* channel

$$\bar{B}(p) \rightarrow \bar{K}^*(k) [\rightarrow \bar{K}(k_1)\pi(k_2)] \ell^+(q_1)\ell^-(q_2) \quad (\text{C.1})$$

where $\bar{K} = \bar{K}^0$ or K^- and $\pi = \pi^+$ or π^0 it is important to define the kinematic variables used since different conventions can be found in the literature. We define ϕ as the angle between the normals to the planes defined by $K^-\pi^+$ and $\ell^+\ell^-$ in the B meson rest frame. The angle θ_ℓ is the angle between the direction of flight of the \bar{B} and the ℓ^- in the dilepton rest frame, and θ_K is the angle between the direction of motion of the \bar{B} and the \bar{K} in the

⁸While we do not present the entire basis here for clarity, `HEPfit` has all of those encoded in it.

dimeson rest frame (note that θ_ℓ and θ_K are defined in the interval $[0, \pi)$). Squaring the amplitude and summing over lepton spins allow us to write the fully differential decay rate as:

$$\begin{aligned} \frac{d^{(4)}\Gamma}{dq^2 d(\cos\theta_\ell) d(\cos\theta_K) d\phi} = & \frac{9}{32\pi} \left(I_1^s \sin^2\theta_K + I_1^c \cos^2\theta_K + (I_2^s \sin^2\theta_K + I_2^c \cos^2\theta_K) \cos 2\theta_\ell \right. \\ & + I_3 \sin^2\theta_K \sin^2\theta_\ell \cos 2\phi + I_4 \sin 2\theta_K \sin 2\theta_\ell \cos \phi \\ & + I_5 \sin 2\theta_K \sin \theta_\ell \cos \phi + (I_6^s \sin^2\theta_K + I_6^c \cos^2\theta_K) \cos \theta_\ell \\ & + I_7 \sin 2\theta_K \sin \theta_\ell \sin \phi + I_8 \sin 2\theta_K \sin 2\theta_\ell \sin \phi \\ & \left. + I_9 \sin^2\theta_K \sin^2\theta_\ell \sin 2\phi \right). \end{aligned} \quad (\text{C.2})$$

The angular coefficients I_i , as functions of q^2 , can be expressed in terms of the helicity amplitudes as⁹

$$\begin{aligned} I_1^c &= F \left(\frac{1}{2} (|H_V^0|^2 + |H_A^0|^2) + |H_P|^2 + \frac{2m_\ell^2}{q^2} (|H_V^0|^2 - |H_A^0|^2) \right), \\ I_1^s &= F \left(\frac{\beta^2 + 2}{8} (|H_V^+|^2 + |H_V^-|^2 + |H_A^+|^2 + |H_A^-|^2) + \frac{m_\ell^2}{q^2} (|H_V^+|^2 - |H_V^-|^2 - |H_A^+|^2 + |H_A^-|^2) \right), \\ I_2^c &= -F \frac{\beta^2}{2} (|H_V^0|^2 + |H_A^0|^2), \\ I_2^s &= F \frac{\beta^2}{8} ((|H_V^+|^2 + |H_V^-|^2) + (|H_A^+|^2 + |H_A^-|^2)), \\ I_3 &= -\frac{F}{2} \text{Re} [H_V^+(H_V^-)^* + H_A^+(H_A^-)^*], \\ I_4 &= F \frac{\beta^2}{4} \text{Re} [(H_V^+ + H_V^-)(H_V^0)^* + (H_A^+ + H_A^-)(H_A^0)^*], \\ I_5 &= F \frac{\beta}{4} \text{Re} [(H_V^- - H_V^+)(H_A^0)^* + (H_A^- - H_A^+)(H_V^0)^*], \\ I_6^s &= F \beta \text{Re} [H_V^-(H_A^-)^* - H_V^+(H_A^+)^*], \\ I_6^c &= 0, \\ I_7 &= F \frac{\beta}{2} \text{Im} [(H_A^+ + H_A^-)(H_V^0)^* + (H_V^+ + H_V^-)(H_A^0)^*], \\ I_8 &= F \frac{\beta^2}{4} \text{Im} [(H_V^- - H_V^+)(H_V^0)^* + (H_A^- - H_A^+)(H_A^0)^*], \\ I_9 &= F \frac{\beta^2}{4} \text{Im} [H_V^+(H_V^-)^* + H_A^+(H_A^-)^*], \end{aligned} \quad (\text{C.3})$$

where

$$\begin{aligned} F &= \frac{\lambda^{1/2} \beta q^2}{3 \times 2^5 \pi^3 m_B^3} \text{BR}(K^* \rightarrow K\pi), \quad \beta = \sqrt{1 - \frac{4m_\ell^2}{q^2}}, \\ \lambda &= m_B^4 + m_V^4 + q^4 - 2(m_B^2 m_V^2 + m_B^2 q^2 + m_V^2 q^2). \end{aligned} \quad (\text{C.4})$$

⁹Again, please note that the angular coefficients are only in terms of the helicity amplitudes that appear in the SM. For the complete expressions see ref. [48].

For the CP-conjugate decay $B \rightarrow K^* \ell^+ \ell^-$, the angular coefficients can be defined by

$$I_{1s(c),2s(c),3,4,7} \rightarrow \bar{I}_{1s(c),2s(c),3,4,7}, \quad I_{5,6s(c),8,9} \rightarrow -\bar{I}_{5,6s(c),8,9}, \quad (\text{C.5})$$

when one uses the angles defined as in the \bar{B} decays with $K^- \rightarrow K^+$ and with conjugated CKM elements.

D Angular observables

From the full angular distribution one can define angular observables in multiple ways. Two different prescriptions have been advocated in the past [10, 27]. While both sets of definitions are equivalent in their physics content, the two different sets have been used for experimental analyses [40–43, 59, 60]. These two definitions can be easily related to each other. Since we shall present our results cast into both sets it is best to define both here.

Following [10], one can define

$$S_i = \frac{I_i + \bar{I}_i}{2\Gamma'}, \quad A_i = \frac{I_i - \bar{I}_i}{2\Gamma'}. \quad (\text{D.1})$$

The twelve q^2 -dependent observables I_i derived in the previous section are all accessible through a full angular analysis of the $\bar{B} \rightarrow \bar{K}^* \ell^+ \ell^-$ decay rate. The analysis of the CP-conjugate decay $B \rightarrow K^* \ell^+ \ell^-$ gives the same number of independent observables, so that it is useful to define the following combinations:

$$\Sigma_i = \frac{I_i + \bar{I}_i}{2}, \quad \Delta_i = \frac{I_i - \bar{I}_i}{2}. \quad (\text{D.2})$$

In an attempt to reduce the uncertainties coming from form factors and hadronic contributions one can define the ratios of the angular coefficients. However, this comes with a caveat. These observables are really “clean” of uncertainties in their analytic functional form and when the form factors are assumed to come with small corrections to the soft form factors in addition to negligible hadronic contributions. In case the latter assumptions break down, which seems to be the most likely case, these observables are no longer “clean” of uncertainties in the form factor and hadronic contributions. Nevertheless, one defines the observables

$$P_1 = \frac{\Sigma_3}{2\Sigma_{2s}}, \quad P_2 = \frac{\Sigma_{6s}}{8\Sigma_{2s}}, \quad P_3 = -\frac{\Sigma_9}{4\Sigma_{2s}}, \quad (\text{D.3})$$

$$P'_4 = \frac{\Sigma_4}{\sqrt{-\Sigma_{2s}\Sigma_{2c}}}, \quad P'_5 = \frac{\Sigma_5}{2\sqrt{-\Sigma_{2s}\Sigma_{2c}}}, \quad P'_6 = -\frac{\Sigma_7}{2\sqrt{-\Sigma_{2s}\Sigma_{2c}}}, \quad P'_8 = -\frac{\Sigma_8}{\sqrt{-\Sigma_{2s}\Sigma_{2c}}}.$$

In addition to these there are the traditional observables, the branching fraction, the longitudinal component and the forward-backward asymmetry which can be defined in terms of the angular coefficients as:

$$\Gamma' = \frac{1}{2} \frac{d\Gamma + d\bar{\Gamma}}{dq^2} = \frac{1}{4} [(3\Sigma_{1c} - \Sigma_{2c}) + 2(3\Sigma_{1s} - \Sigma_{2s})],$$

$$F_L = \frac{3\Sigma_{1c} - \Sigma_{2c}}{4\Gamma'}, \quad A_{FB} = -\frac{3\Sigma_{6s}}{4\Gamma'}. \quad (\text{D.4})$$

In the limit $q^2 \gg m_\ell^2$ the terms proportional to m_ℓ^2/q^2 can be dropped from the angular coefficients in eq. (C.3) and the helicity amplitude $H_P \rightarrow 0$ since it is proportional to m_i/q^2 . In this limit there are further relations connecting the angular coefficients effectively reducing the number of independent observables. These relations can be written as:

$$\Sigma_{1c} = -\Sigma_{2c} \quad \text{and} \quad \Sigma_{1s} = 3\Sigma_{2s}. \quad (\text{D.5})$$

This simplifies the expressions for F_L and Γ' to

$$F_L = \frac{\Sigma_{1c}}{\Gamma'} \quad \text{and} \quad \Gamma' = \Sigma_{1c} + 4\Sigma_{2s}. \quad (\text{D.6})$$

Experimentally the observables are measured in binned data cut in regions of q^2 , the dilepton invariant mass. The translation of the analytic expressions to the experimentally binned observables is as follows:

$$\begin{aligned} \langle P_1 \rangle &= \frac{\langle \Sigma_3 \rangle}{2 \langle \Sigma_{2s} \rangle}, & \langle P_2 \rangle &= \frac{\langle \Sigma_{6s} \rangle}{8 \langle \Sigma_{2s} \rangle}, & \langle P_3 \rangle &= -\frac{\langle \Sigma_9 \rangle}{4 \langle \Sigma_{2s} \rangle}, \\ \langle P'_4 \rangle &= \frac{\langle \Sigma_4 \rangle}{\sqrt{-\langle \Sigma_{2s} \Sigma_{2c} \rangle}}, & \langle P'_5 \rangle &= \frac{\langle \Sigma_5 \rangle}{2\sqrt{-\langle \Sigma_{2s} \Sigma_{2c} \rangle}}, \\ \langle P'_6 \rangle &= -\frac{\langle \Sigma_7 \rangle}{2\sqrt{-\langle \Sigma_{2s} \Sigma_{2c} \rangle}}, & \langle P'_8 \rangle &= -\frac{\langle \Sigma_8 \rangle}{2\sqrt{-\langle \Sigma_{2s} \Sigma_{2c} \rangle}}, \end{aligned} \quad (\text{D.7})$$

where it should be noted that the ratio of the binned angular coefficients are the relevant rather than the binned ratios since:

$$\langle \Sigma_i \rangle = \int_{q_{min}^2}^{q_{max}^2} \Sigma_i(q^2) dq^2. \quad (\text{D.8})$$

Furthermore, the binned branching fraction, F_L and A_{FB} are defined as:

$$\langle \Gamma' \rangle = \langle \Sigma_{1c} + 4\Sigma_{2s} \rangle, \quad \langle F_L \rangle = \frac{\langle 3\Sigma_{1c} - \Sigma_{2c} \rangle}{4 \langle \Gamma' \rangle}, \quad \langle A_{FB} \rangle = -\frac{3 \langle \Sigma_{6s} \rangle}{4 \langle \Gamma' \rangle}. \quad (\text{D.9})$$

Even though the angular observables built out of the angular coefficients are measured over bins as we have described, in effect defeating some of the purpose of being clean that they were originally advocated for, it is informative to take a look at their analytic form assuming only SM contributions being present. The extension to the full expressions will not be presented here as the expressions become quite lengthy. The simplified forms are given by:

$$P_1 = -\frac{2}{1 - 4\frac{m_\ell^2}{q^2}} \frac{\text{Re}[(C_{10}V_+)(C_{10}V_-)^*] + \text{Re}[D_+D_-^*]}{|C_{10}V_-|^2 + |C_{10}V_+|^2 + |D_+|^2 + |D_-|^2}, \quad (\text{D.10})$$

$$P_2 = \frac{1}{\sqrt{1 - 4\frac{m_\ell^2}{q^2}}} \frac{\text{Re}[D_+(C_{10}V_+)^* + D_-(C_{10}V_-)^*]}{|C_{10}V_-|^2 + |C_{10}V_+|^2 + |D_+|^2 + |D_-|^2}, \quad (\text{D.11})$$

$$P_3 = -\frac{\text{Im}[(C_{10}V_+)(C_{10}V_-)^*] + \text{Im}[D_+D_-^*]}{|C_{10}V_-|^2 + |C_{10}V_+|^2 + |D_+|^2 + |D_-|^2}, \quad (\text{D.12})$$

$$P'_4 = \frac{\text{Re}[C_{10}(V_- + V_+)(C_{10}\tilde{V}_0)^*] + \text{Re}[(D_- + D_+)D_0^*]}{\sqrt{\left(|C_{10}\tilde{V}_0|^2 + |D_0|^2\right) \left(|C_{10}V_-|^2 + |C_{10}V_+|^2 + |D_+|^2 + |D_-|^2\right)}}, \quad (\text{D.13})$$

$$P'_5 = -\frac{\text{Re}[(D_- - D_+)(C_{10}\tilde{V}_0)^*] + \text{Re}[C_{10}(V_- - V_+)(D_0)^*]}{\sqrt{\left(1 - \frac{4m_c^2}{q^2}\right) \left(|C_{10}\tilde{V}_0|^2 + |D_0|^2\right) \left(|C_{10}V_-|^2 + |C_{10}V_+|^2 + |D_+|^2 + |D_-|^2\right)}}, \quad (\text{D.14})$$

$$P'_6 = -\frac{\text{Im}[(D_- - D_+)(C_{10}\tilde{V}_0)^*] + \text{Im}[C_{10}(V_- - V_+)D_0^*]}{\sqrt{\left(1 - \frac{4m_c^2}{q^2}\right) \left(|C_{10}\tilde{V}_0|^2 + |D_0|^2\right) \left(|C_{10}V_-|^2 + |C_{10}V_+|^2 + |D_+|^2 + |D_-|^2\right)}}, \quad (\text{D.15})$$

$$P'_8 = \frac{\text{Im}[C_{10}(V_- - V_+)(C_{10}\tilde{V}_0)^*] + \text{Im}[(D_- - D_+)D_0^*]}{\sqrt{\left(|C_{10}\tilde{V}_0|^2 + |D_0|^2\right) \left(|C_{10}V_-|^2 + |C_{10}V_+|^2 + |D_+|^2 + |D_-|^2\right)}}, \quad (\text{D.16})$$

where

$$\begin{aligned} D_0 &= \frac{m_B^2}{q^2} \left(16\pi^2 h_0(q^2) - 2\frac{m_b}{m_B} C_7^{\text{eff}} \tilde{T}_0 \right) - C_9^{\text{eff}}(q^2) \tilde{V}_0, \\ D_+ &= \frac{m_B^2}{q^2} \left(16\pi^2 h_+(q^2) - 2\frac{m_b}{m_B} C_7^{\text{eff}} T_+ \right) - C_9^{\text{eff}}(q^2) V_+, \\ D_- &= \frac{m_B^2}{q^2} \left(16\pi^2 h_-(q^2) - 2\frac{m_b}{m_B} C_7^{\text{eff}} T_- \right) - C_9^{\text{eff}}(q^2) V_-, \end{aligned} \quad (\text{D.17})$$

which are proportional to H_V^λ given in eq. (B.1). In the SM C_7^{eff} and C_{10} do not pick up any q^2 dependence at low energy and remain purely real. $C_9^{\text{eff}}(q^2)$ is defined as

$$C_9^{\text{eff}}(q^2) = C_9^{\text{eff}} + Y(q^2), \quad (\text{D.18})$$

where $Y(q^2)$ comes from the perturbative part of the charm loop contribution [6, 81, 82]. We emphasize that we do not include the latter contribution in our definition for h_λ since it contains non-factorizable contributions only.

It is instrumental at this point to underline the connection between the two different sets of observables that are generally advocated in the literature. There are some simple relations between them in the $q^2 \gg m_c^2$ limit. While this limit does not strictly hold in the lower q^2 region it does provide some insight into the way these sets are connected so we shall collect the formula here [27, 29].

$$\begin{aligned}
P_1 = A_T^{(2)} &= \frac{2S_3}{1 - F_L}, & P_2 &= -\frac{2}{3} \frac{A_{FB}}{1 - F_L}, & P_3 &= -\frac{S_9}{1 - F_L} \\
P'_4 &= \frac{2S_4}{\sqrt{F_L(1 - F_L)}}, & P'_5 &= \frac{S_5}{\sqrt{F_L(1 - F_L)}}, & P'_6 &= -\frac{S_7}{\sqrt{F_L(1 - F_L)}}, \\
P'_8 &= -\frac{2S_8}{\sqrt{F_L(1 - F_L)}}. & & & &
\end{aligned} \tag{D.19}$$

In all the above relations, both the left and the right hand sides pertain to the definitions of the kinematic variables used in theory computations. It should also be noted that due to the difference in the definitions of the kinematic variable between the convention used for theory calculation and for experimental measurements at the LHCb, the numerical results between the two are connected by [21, 79]:

$$P_2^{\text{LHCb}} = -P_2^{\text{T}}, \quad P_3^{\text{LHCb}} = -P_3^{\text{T}}, \quad P_4^{\text{LHCb}} = -\frac{1}{2}P_4^{\text{T}} \quad \text{and} \quad P_8^{\text{LHCb}} = -\frac{1}{2}P_8^{\text{T}}, \tag{D.20}$$

where the superscript T implies theory definitions. While the sign difference stems from the change in the definition of the kinematic variables the factors of two come from the difference in the definitions of the variables themselves.

E Tests and Cross-checks

As explained in section 3, we performed several tests and cross-checks to assess the dependence of our results on our assumptions on the size and shape of nonfactorizable power corrections.

As a first test, we performed our fit without using the numerical information from ref. [47]. The results of the fit for the $B \rightarrow K^* \mu^+ \mu^-$ observables are reported in table 7, while the ones for the $B \rightarrow K^* e^+ e^-$ observables are in table 10. Plots for the $B \rightarrow K^* \mu^+ \mu^-$ angular observables are shown in figure 5.

As a further test, we performed our fit adopting the phenomenological model of ref. [47] for the q^2 dependence of the power corrections, although we consider this model to be inadequate for $q^2 \sim 4m_c^2$ as discussed in section 2. The results for the $B \rightarrow K^* \mu^+ \mu^-$ observables are reported in table 8, while the ones for the $B \rightarrow K^* e^+ e^-$ observables are in table 11. Plots for the $B \rightarrow K^* \mu^+ \mu^-$ angular observables are shown in figure 6.

Finally, we performed our fit assuming vanishing $h_\lambda^{(2)}$, i.e. hadronic corrections fully equivalent to a shift in $C_{7,9}$. The results for the $B \rightarrow K^* \mu^+ \mu^-$ observables are reported in table 9, while the ones for the $B \rightarrow K^* e^+ e^-$ observables are in table 12. Plots for the $B \rightarrow K^* \mu^+ \mu^-$ angular observables are shown in figure 7.

See section 3 for a discussion of the physical implications of the results reported here.

q^2 bin [GeV ²]	Observable	measurement	full fit	prediction	p – value
[0.1, 0.98]	F_L	0.264 ± 0.048	0.274 ± 0.036	0.255 ± 0.037	0.14
	S_3	-0.036 ± 0.063	-0.017 ± 0.026	-0.021 ± 0.037	
	S_4	0.082 ± 0.069	0.033 ± 0.045	-0.032 ± 0.049	
	S_5	0.170 ± 0.061	0.259 ± 0.029	0.261 ± 0.040	
	A_{FB}	-0.003 ± 0.058	-0.098 ± 0.009	-0.092 ± 0.012	
	S_7	0.015 ± 0.059	-0.031 ± 0.055	-0.119 ± 0.072	
	S_8	0.080 ± 0.076	0.030 ± 0.049	-0.008 ± 0.045	
	S_9	-0.082 ± 0.058	-0.020 ± 0.026	-0.007 ± 0.028	
	P'_5	0.387 ± 0.142	0.740 ± 0.096	0.760 ± 0.120	
	[1.1, 2.5]	F_L	0.663 ± 0.083	0.668 ± 0.039	0.664 ± 0.046
S_3		-0.086 ± 0.096	-0.017 ± 0.032	-0.009 ± 0.033	
S_4		-0.078 ± 0.112	-0.055 ± 0.037	-0.061 ± 0.039	
S_5		0.140 ± 0.097	0.170 ± 0.052	0.186 ± 0.064	
A_{FB}		-0.197 ± 0.075	-0.195 ± 0.023	-0.194 ± 0.026	
S_7		-0.224 ± 0.099	-0.077 ± 0.063	0.020 ± 0.078	
S_8		-0.106 ± 0.116	0.014 ± 0.040	0.034 ± 0.040	
S_9		-0.128 ± 0.096	-0.028 ± 0.036	-0.014 ± 0.036	
P'_5		0.298 ± 0.212	0.370 ± 0.110	0.410 ± 0.140	0.66
[2.5, 4]		F_L	0.882 ± 0.104	0.725 ± 0.033	0.700 ± 0.041
	S_3	0.040 ± 0.094	-0.016 ± 0.017	-0.024 ± 0.023	
	S_4	-0.242 ± 0.136	-0.167 ± 0.029	-0.167 ± 0.033	
	S_5	-0.019 ± 0.107	-0.055 ± 0.054	-0.066 ± 0.066	
	A_{FB}	-0.122 ± 0.086	-0.093 ± 0.031	-0.091 ± 0.037	
	S_7	0.072 ± 0.116	-0.066 ± 0.059	-0.113 ± 0.072	
	S_8	0.029 ± 0.130	0.005 ± 0.032	0.005 ± 0.034	
	S_9	-0.102 ± 0.115	-0.011 ± 0.018	-0.015 ± 0.023	
	P'_5	-0.077 ± 0.354	-0.130 ± 0.120	-0.150 ± 0.150	0.85
	[4, 6]	F_L	0.610 ± 0.055	0.652 ± 0.031	0.667 ± 0.036
S_3		0.036 ± 0.069	-0.027 ± 0.017	-0.028 ± 0.018	
S_4		-0.218 ± 0.085	-0.235 ± 0.017	-0.232 ± 0.020	
S_5		-0.146 ± 0.078	-0.182 ± 0.044	-0.204 ± 0.052	
A_{FB}		0.024 ± 0.052	0.042 ± 0.030	0.060 ± 0.037	
S_7		-0.016 ± 0.081	-0.039 ± 0.049	-0.047 ± 0.062	
S_8		0.168 ± 0.093	-0.005 ± 0.030	-0.023 ± 0.030	
S_9		-0.032 ± 0.071	-0.006 ± 0.015	-0.011 ± 0.016	
P'_5		-0.301 ± 0.160	-0.386 ± 0.093	-0.440 ± 0.110	0.47
[6, 8]		F_L	0.579 ± 0.048	0.569 ± 0.035	0.516 ± 0.075
	S_3	-0.042 ± 0.060	-0.046 ± 0.031	0.005 ± 0.060	
	S_4	-0.298 ± 0.066	-0.262 ± 0.018	-0.213 ± 0.040	
	S_5	-0.250 ± 0.061	-0.238 ± 0.050	-0.160 ± 0.110	
	A_{FB}	0.152 ± 0.041	0.148 ± 0.036	0.107 ± 0.080	
	S_7	-0.046 ± 0.067	-0.028 ± 0.056	0.040 ± 0.120	
	S_8	-0.084 ± 0.071	-0.017 ± 0.040	0.043 ± 0.058	
	S_9	-0.024 ± 0.060	-0.013 ± 0.033	0.020 ± 0.055	
	P'_5	-0.505 ± 0.124	-0.490 ± 0.100	-0.320 ± 0.230	0.48
	[0.1, 2]	BR $\cdot 10^7$	0.58 ± 0.09	0.67 ± 0.04	0.70 ± 0.06
[2, 4.3]	0.29 ± 0.05		0.34 ± 0.03	0.37 ± 0.05	0.26
[4.3, 8.68]	0.47 ± 0.07		0.46 ± 0.06	0.49 ± 0.13	0.89
	BR $_{B \rightarrow K^* \gamma} \cdot 10^5$	4.33 ± 0.15	4.34 ± 0.15	4.59 ± 0.77	0.74

Table 7. Experimental results, results from the full fit, predictions and p-values for $B \rightarrow K^* \mu^+ \mu^-$ BR's and angular observables obtained without using the numerical information from ref. [47]. The predictions for the BR's (angular observables) are obtained removing the corresponding observable (the experimental information in one bin at a time) from the fit. We also report the results for BR($B \rightarrow K^* \gamma$) (including the experimental value from refs. [65, 73–75]) and for the optimized observable P'_5 . The latter is however not explicitly used in the fit as a constraint, since it is not independent of F_L and S_5 .

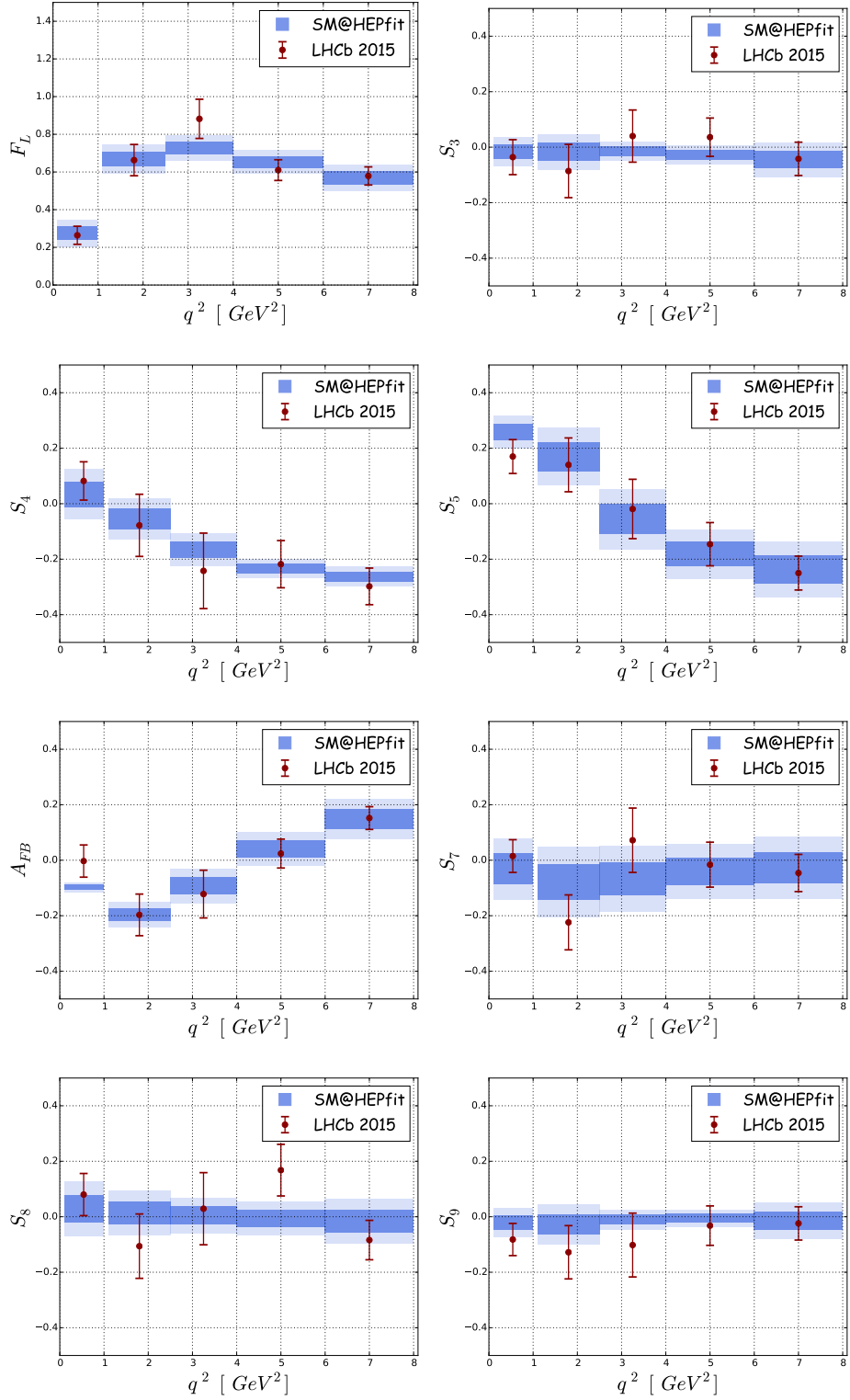


Figure 5. Results of the full fit and experimental results for the $B \rightarrow K^* \mu^+ \mu^-$ angular observables obtained without using the numerical information from ref. [47].

q^2 bin [GeV ²]	Observable	measurement	full fit	prediction	p – value
[0.1, 0.98]	F_L	0.264 ± 0.048	0.270 ± 0.032	0.257 ± 0.025	0.056
	S_3	-0.036 ± 0.063	0.004 ± 0.004	0.004 ± 0.004	
	S_4	0.082 ± 0.069	0.010 ± 0.048	-0.047 ± 0.035	
	S_5	0.170 ± 0.061	0.293 ± 0.024	0.314 ± 0.015	
	A_{FB}	-0.003 ± 0.058	-0.101 ± 0.005	-0.102 ± 0.005	
	S_7	0.015 ± 0.059	-0.046 ± 0.015	-0.041 ± 0.014	
	S_8	0.080 ± 0.076	0.023 ± 0.045	-0.005 ± 0.036	
	S_9	-0.082 ± 0.058	-0.001 ± 0.003	-0.001 ± 0.003	
	P'_5	0.387 ± 0.142	0.840 ± 0.088	0.919 ± 0.051	
	[1.1, 2.5]	F_L	0.663 ± 0.083	0.711 ± 0.024	0.711 ± 0.027
S_3		-0.086 ± 0.096	0.001 ± 0.003	0.001 ± 0.003	
S_4		-0.078 ± 0.112	-0.073 ± 0.020	-0.078 ± 0.022	
S_5		0.140 ± 0.097	0.190 ± 0.039	0.201 ± 0.043	
A_{FB}		-0.197 ± 0.075	-0.185 ± 0.016	-0.186 ± 0.017	
S_7		-0.224 ± 0.099	-0.061 ± 0.030	-0.050 ± 0.032	
S_8		-0.106 ± 0.116	-0.010 ± 0.021	-0.014 ± 0.021	
S_9		-0.128 ± 0.096	-0.002 ± 0.003	-0.001 ± 0.003	
P'_5		0.298 ± 0.212	0.434 ± 0.082	0.458 ± 0.090	0.49
[2.5, 4]		F_L	0.882 ± 0.104	0.770 ± 0.020	0.767 ± 0.021
	S_3	0.040 ± 0.094	-0.016 ± 0.004	-0.017 ± 0.004	
	S_4	-0.242 ± 0.136	-0.187 ± 0.012	-0.188 ± 0.013	
	S_5	-0.019 ± 0.107	-0.112 ± 0.029	-0.119 ± 0.030	
	A_{FB}	-0.122 ± 0.086	-0.034 ± 0.011	-0.032 ± 0.012	
	S_7	0.072 ± 0.116	-0.029 ± 0.030	-0.035 ± 0.030	
	S_8	0.029 ± 0.130	-0.013 ± 0.006	-0.012 ± 0.006	
	S_9	-0.102 ± 0.115	-0.002 ± 0.001	-0.002 ± 0.001	
	P'_5	-0.077 ± 0.354	-0.271 ± 0.072	-0.287 ± 0.074	0.56
	[4, 6]	F_L	0.610 ± 0.055	0.679 ± 0.024	0.682 ± 0.026
S_3		0.036 ± 0.069	-0.036 ± 0.008	-0.035 ± 0.009	
S_4		-0.218 ± 0.085	-0.249 ± 0.008	-0.247 ± 0.009	
S_5		-0.146 ± 0.078	-0.295 ± 0.021	-0.312 ± 0.021	
A_{FB}		0.024 ± 0.052	0.139 ± 0.014	0.146 ± 0.016	
S_7		-0.016 ± 0.081	-0.002 ± 0.026	-0.002 ± 0.026	
S_8		0.168 ± 0.093	-0.006 ± 0.005	-0.006 ± 0.005	
S_9		-0.032 ± 0.071	-0.002 ± 0.002	-0.002 ± 0.002	
P'_5		-0.301 ± 0.160	-0.637 ± 0.047	-0.676 ± 0.047	0.025
[6, 8]		F_L	0.579 ± 0.048	0.585 ± 0.029	0.561 ± 0.038
	S_3	-0.042 ± 0.060	-0.054 ± 0.011	-0.053 ± 0.013	
	S_4	-0.298 ± 0.066	-0.271 ± 0.007	-0.271 ± 0.007	
	S_5	-0.250 ± 0.061	-0.383 ± 0.017	-0.392 ± 0.019	
	A_{FB}	0.152 ± 0.041	0.264 ± 0.019	0.286 ± 0.025	
	S_7	-0.046 ± 0.067	-0.000 ± 0.036	0.021 ± 0.039	
	S_8	-0.084 ± 0.071	-0.001 ± 0.010	0.005 ± 0.011	
	S_9	-0.024 ± 0.060	-0.001 ± 0.004	-0.000 ± 0.005	
	P'_5	-0.505 ± 0.124	-0.783 ± 0.038	-0.797 ± 0.041	0.025
	[0.1, 2]	BR $\cdot 10^7$	0.58 ± 0.09	0.64 ± 0.03	0.65 ± 0.04
[2, 4.3]	0.29 ± 0.05		0.33 ± 0.03	0.35 ± 0.03	0.30
[4.3, 8.68]	0.47 ± 0.07		0.48 ± 0.04	0.49 ± 0.05	0.82
	BR $_{B \rightarrow K^* \gamma} \cdot 10^5$	4.33 ± 0.15	4.35 ± 0.14	4.69 ± 0.53	0.51

Table 8. Experimental results, results from the full fit, predictions and p-values for $B \rightarrow K^* \mu^+ \mu^-$ BR's and angular observables obtained using the phenomenological model from ref. [47]. The predictions for the BR's (angular observables) are obtained removing the corresponding observable (the experimental information in one bin at a time) from the fit. We also report the results for BR($B \rightarrow K^* \gamma$) (including the experimental value from refs. [65, 73–75]) and for the optimized observable P'_5 . The latter is however not explicitly used in the fit as a constraint, since it is not independent of F_L and S_5 .

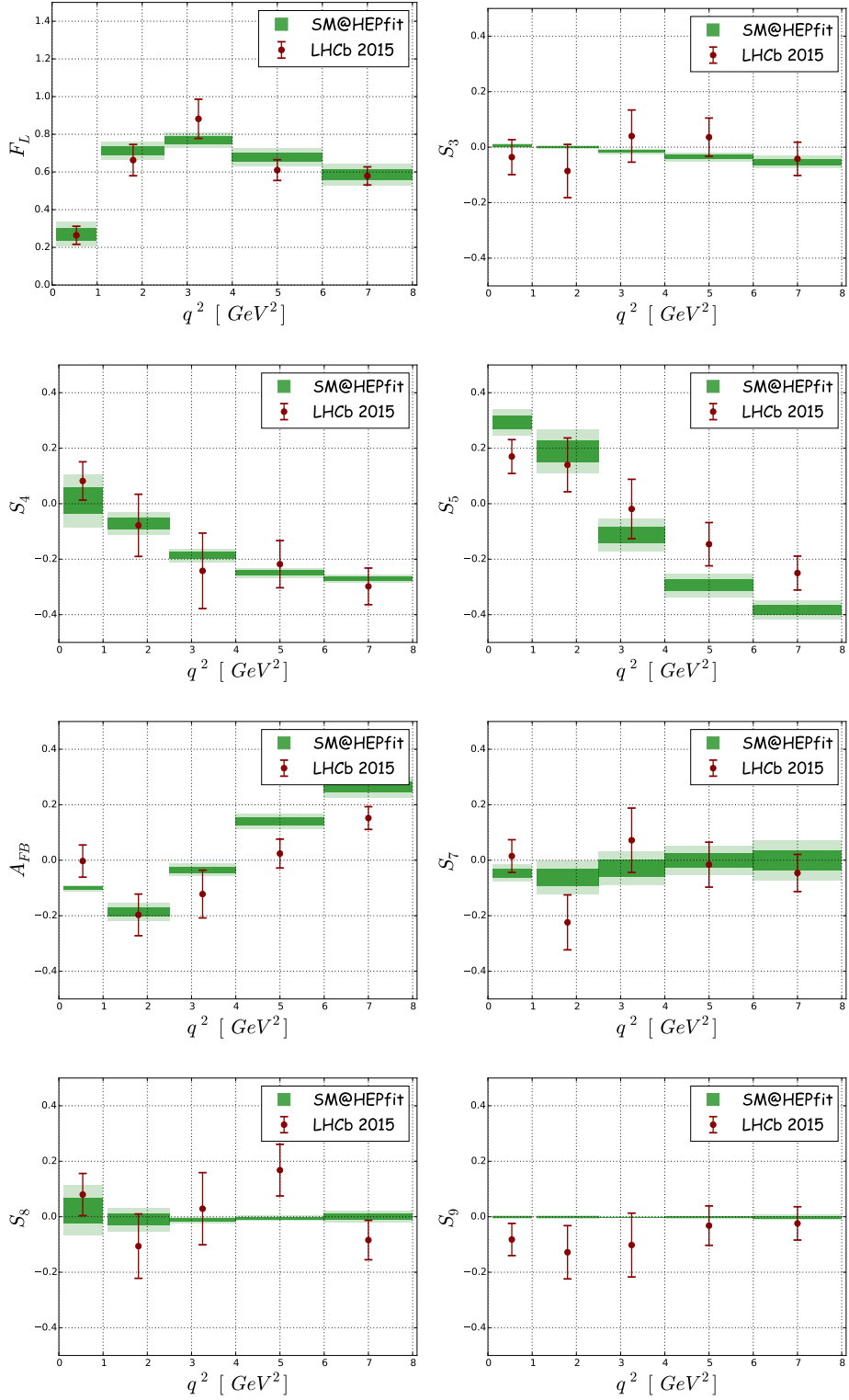


Figure 6. Results of the full fit and experimental results for the $B \rightarrow K^* \mu^+ \mu^-$ angular observables obtained using the phenomenological model from ref. [47].

q^2 bin [GeV ²]	Observable	measurement	full fit	prediction	p – value
[0.1, 0.98]	F_L	0.264 ± 0.048	0.272 ± 0.034	0.251 ± 0.033	0.11
	S_3	-0.036 ± 0.063	0.004 ± 0.007	0.004 ± 0.008	
	S_4	0.082 ± 0.069	0.039 ± 0.040	-0.024 ± 0.045	
	S_5	0.170 ± 0.061	0.274 ± 0.027	0.305 ± 0.023	
	A_{FB}	-0.003 ± 0.058	-0.104 ± 0.006	-0.106 ± 0.006	
	S_7	0.015 ± 0.059	-0.047 ± 0.015	-0.041 ± 0.016	
	S_8	0.080 ± 0.076	0.028 ± 0.049	-0.003 ± 0.046	
	S_9	-0.082 ± 0.058	-0.001 ± 0.007	-0.002 ± 0.007	
	P'_5	0.387 ± 0.142	0.782 ± 0.093	0.896 ± 0.080	
	[1.1, 2.5]	F_L	0.663 ± 0.083	0.662 ± 0.029	0.656 ± 0.033
S_3		-0.086 ± 0.096	0.005 ± 0.011	0.006 ± 0.012	
S_4		-0.078 ± 0.112	-0.048 ± 0.023	-0.060 ± 0.027	
S_5		0.140 ± 0.097	0.214 ± 0.040	0.238 ± 0.046	
A_{FB}		-0.197 ± 0.075	-0.216 ± 0.019	-0.221 ± 0.021	
S_7		-0.224 ± 0.099	-0.078 ± 0.035	-0.064 ± 0.038	
S_8		-0.106 ± 0.116	0.007 ± 0.031	0.010 ± 0.032	
S_9		-0.128 ± 0.096	-0.003 ± 0.012	0.001 ± 0.013	
P'_5		0.298 ± 0.212	0.468 ± 0.085	0.519 ± 0.097	0.34
[2.5, 4]		F_L	0.882 ± 0.104	0.731 ± 0.023	0.721 ± 0.025
	S_3	0.040 ± 0.094	-0.010 ± 0.007	-0.011 ± 0.007	
	S_4	-0.242 ± 0.136	-0.166 ± 0.017	-0.166 ± 0.018	
	S_5	-0.019 ± 0.107	-0.023 ± 0.041	-0.021 ± 0.045	
	A_{FB}	-0.122 ± 0.086	-0.113 ± 0.024	-0.119 ± 0.025	
	S_7	0.072 ± 0.116	-0.064 ± 0.039	-0.080 ± 0.041	
	S_8	0.029 ± 0.130	-0.003 ± 0.022	-0.005 ± 0.023	
	S_9	-0.102 ± 0.115	-0.003 ± 0.008	-0.004 ± 0.008	
	P'_5	-0.077 ± 0.354	-0.054 ± 0.095	-0.050 ± 0.100	0.94
	[4, 6]	F_L	0.610 ± 0.055	0.662 ± 0.025	0.678 ± 0.028
S_3		0.036 ± 0.069	-0.031 ± 0.009	-0.033 ± 0.010	
S_4		-0.218 ± 0.085	-0.238 ± 0.013	-0.236 ± 0.015	
S_5		-0.146 ± 0.078	-0.193 ± 0.043	-0.234 ± 0.049	
A_{FB}		0.024 ± 0.052	0.049 ± 0.028	0.076 ± 0.035	
S_7		-0.016 ± 0.081	-0.039 ± 0.045	-0.045 ± 0.054	
S_8		0.168 ± 0.093	-0.005 ± 0.017	-0.012 ± 0.018	
S_9		-0.032 ± 0.071	-0.002 ± 0.006	-0.004 ± 0.007	
P'_5		-0.301 ± 0.160	-0.413 ± 0.093	-0.510 ± 0.110	0.28
[6, 8]		F_L	0.579 ± 0.048	0.574 ± 0.030	0.552 ± 0.043
	S_3	-0.042 ± 0.060	-0.054 ± 0.015	-0.051 ± 0.018	
	S_4	-0.298 ± 0.066	-0.268 ± 0.010	-0.261 ± 0.017	
	S_5	-0.250 ± 0.061	-0.302 ± 0.037	-0.311 ± 0.055	
	A_{FB}	0.152 ± 0.041	0.200 ± 0.029	0.245 ± 0.043	
	S_7	-0.046 ± 0.067	-0.029 ± 0.050	0.014 ± 0.077	
	S_8	-0.084 ± 0.071	-0.001 ± 0.017	0.010 ± 0.023	
	S_9	-0.024 ± 0.060	0.002 ± 0.012	0.006 ± 0.015	
	P'_5	-0.505 ± 0.124	-0.616 ± 0.077	-0.630 ± 0.110	0.45
	[0.1, 2]	BR $\cdot 10^7$	0.58 ± 0.09	0.69 ± 0.04	0.71 ± 0.04
[2, 4.3]	0.29 ± 0.05		0.34 ± 0.02	0.36 ± 0.03	0.23
[4.3, 8.68]	0.47 ± 0.07		0.44 ± 0.04	0.43 ± 0.04	0.62
	BR $_{B \rightarrow K^* \gamma} \cdot 10^5$	4.33 ± 0.15	4.32 ± 0.14	4.30 ± 0.48	0.95

Table 9. Experimental results, results from the full fit, predictions and p-values for $B \rightarrow K^* \mu^+ \mu^-$ BR's and angular observables obtained assuming vanishing $h_\lambda^{(2)}$, i.e. hadronic corrections fully equivalent to a shift in $C_{7,9}$. The predictions for the BR's (angular observables) are obtained removing the corresponding observable (the experimental information in one bin at a time) from the fit. We also report the results for $BR(B \rightarrow K^* \gamma)$ (including the experimental value from refs. [65, 73–75]) and for the optimized observable P'_5 . The latter is however not explicitly used in the fit as a constraint, since it is not independent of F_L and S_5 .

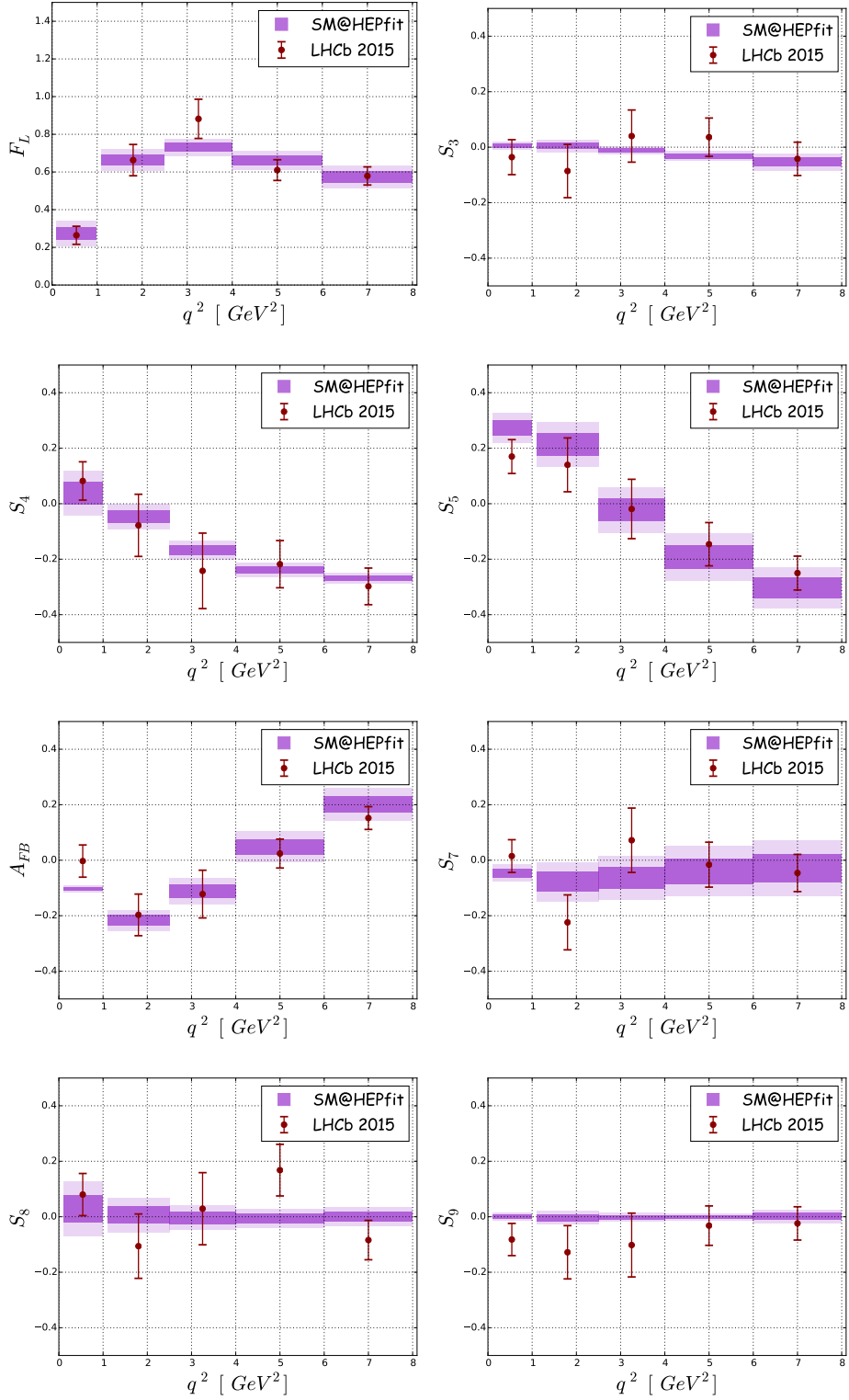


Figure 7. Results of the full fit and experimental results for the $B \rightarrow K^* \mu^+ \mu^-$ angular observables obtained assuming vanishing $h_\lambda^{(2)}$, i.e. hadronic corrections fully equivalent to a shift in $C_{7,9}$.

Observable	measurement	full fit	prediction	p-value
P_1	-0.23 ± 0.24	-0.040 ± 0.07	-0.03 ± 0.07	0.42
P_2	0.05 ± 0.09	-0.040 ± 0.00	-0.040 ± 0.00	0.32
P_3	-0.07 ± 0.11	0.02 ± 0.03	0.03 ± 0.04	0.39
F_L	0.16 ± 0.08	0.170 ± 0.04	0.18 ± 0.05	0.82
$\text{BR} \cdot 10^7$	3.1 ± 1.0	1.4 ± 0.1	1.4 ± 0.1	0.06

Table 10. Experimental results (with symmetrized errors), results from the full fit, predictions and p-values for $B \rightarrow K^*e^+e^-$ BR and angular observables obtained without using the numerical information from ref. [47]. The predictions are obtained removing the corresponding observable from the fit.

Observable	measurement	full fit	prediction	p-value
P_1	-0.23 ± 0.24	0.01 ± 0.01	0.01 ± 0.01	0.32
P_2	0.05 ± 0.09	-0.040 ± 0.00	-0.040 ± 0.00	0.32
P_3	-0.07 ± 0.11	0.00 ± 0.01	0.00 ± 0.01	0.53
F_L	0.16 ± 0.08	0.18 ± 0.04	0.20 ± 0.060	0.66
$\text{BR} \cdot 10^7$	3.1 ± 1.0	1.4 ± 0.1	1.4 ± 0.1	0.06

Table 11. Experimental results (with symmetrized errors), results from the full fit, predictions and p-values for $B \rightarrow K^*e^+e^-$ BR and angular observables obtained using the phenomenological model from ref. [47]. The predictions are obtained removing the corresponding observable from the fit.

Observable	measurement	full fit	prediction	p-value
P_1	-0.23 ± 0.24	0.00 ± 0.02	0.01 ± 0.02	0.32
P_2	0.05 ± 0.09	-0.05 ± 0.00	-0.05 ± 0.00	0.27
P_3	-0.07 ± 0.11	0.00 ± 0.01	0.00 ± 0.01	0.53
F_L	0.16 ± 0.08	0.170 ± 0.04	0.170 ± 0.05	0.91
$\text{BR} \cdot 10^7$	3.1 ± 1.0	1.4 ± 0.1	1.4 ± 0.1	0.06

Table 12. Experimental results (with symmetrized errors), results from the full fit, predictions and p-values for $B \rightarrow K^*e^+e^-$ BR and angular observables obtained assuming vanishing $h_\chi^{(2)}$, i.e. hadronic corrections fully equivalent to a shift in $C_{7,9}$. The predictions are obtained removing the corresponding observable from the fit.

References

- [1] G. Eilam, A. Soni, G. L. Kane, and N. Deshpande, $B \rightarrow K\ell^+\ell^-$ and Other Rare B Meson Decays, *Phys.Rev.Lett.* **57** (1986) 1106.
- [2] W.-S. Hou, R. Willey, and A. Soni, Implications of a Heavy Top Quark and a Fourth Generation on the Decays $B \rightarrow K\ell^+\ell^-$, K Neutrino anti-neutrino, *Phys.Rev.Lett.* **58** (1987) 1608.
- [3] R. Godbole, U. Turke, and M. Wirbel, $B \rightarrow K\mu^+\mu^-$: Light Higgs and Fourth Generation, *Phys.Lett.* **B194** (1987) 302.

- [4] W.-S. Hou and R. Willey, *Effects of Charged Higgs Bosons on the Processes $b \rightarrow s\gamma$, $b \rightarrow sg^*$ and $b \rightarrow s\ell^+\ell^-$* , *Phys.Lett.* **B202** (1988) 591.
- [5] N. Deshpande and J. Trampetic, *Improved Estimates for Processes $b \rightarrow se^+e^-$, $B \rightarrow Ke^+e^-$ and $B \rightarrow K^*e^+e^-$* , *Phys.Rev.Lett.* **60** (1988) 2583.
- [6] B. Grinstein, M. J. Savage, and M. B. Wise, *$B \rightarrow X(s)e^+e^-$ in the Six Quark Model*, *Nucl.Phys.* **B319** (1989) 271–290.
- [7] X. He, T. Nguyen, and R. Volkas, *B Meson Rare Decays in Two Higgs Doublets Models*, *Phys.Rev.* **D38** (1988) 814.
- [8] M. Ciuchini, *Effects of the Charged Higgs Boson on the $b \rightarrow s\ell^+\ell^-$ Decay*, *Mod.Phys.Lett.* **A4** (1989) 1945.
- [9] P. Colangelo, F. De Fazio, P. Santorelli, and E. Scrimieri, *QCD sum rule analysis of the decays $B \rightarrow K\ell^+\ell^-$ and $B \rightarrow K^*\ell^+\ell^-$* , *Phys.Rev.* **D53** (1996) 3672–3686, [[hep-ph/9510403](#)].
- [10] W. Altmannshofer, P. Ball, A. Bharucha, A. J. Buras, D. M. Straub, et al., *Symmetries and Asymmetries of $B \rightarrow K^*\mu^+\mu^-$ Decays in the Standard Model and Beyond*, *JHEP* **0901** (2009) 019, [[arXiv:0811.1214](#)].
- [11] M. Beneke and T. Feldmann, *Symmetry breaking corrections to heavy to light B meson form-factors at large recoil*, *Nucl.Phys.* **B592** (2001) 3–34, [[hep-ph/0008255](#)].
- [12] M. Beneke, T. Feldmann, and D. Seidel, *Systematic approach to exclusive $B \rightarrow V\ell^+\ell^-$, V gamma decays*, *Nucl.Phys.* **B612** (2001) 25–58, [[hep-ph/0106067](#)].
- [13] B. Grinstein and D. Pirjol, *Exclusive rare $B \rightarrow K^*\ell^+\ell^-$ decays at low recoil: Controlling the long-distance effects*, *Phys.Rev.* **D70** (2004) 114005, [[hep-ph/0404250](#)].
- [14] C. Bobeth, G. Hiller, and D. van Dyk, *The Benefits of $\bar{B}^- \rightarrow \bar{K}^*\ell^+\ell^-$ Decays at Low Recoil*, *JHEP* **1007** (2010) 098, [[arXiv:1006.5013](#)].
- [15] M. Beylich, G. Buchalla, and T. Feldmann, *Theory of $B \rightarrow K^{(*)}\ell^+\ell^-$ decays at high q^2 : OPE and quark-hadron duality*, *Eur.Phys.J.* **C71** (2011) 1635, [[arXiv:1101.5118](#)].
- [16] C. Bobeth, G. Hiller, and D. van Dyk, *More Benefits of Semileptonic Rare B Decays at Low Recoil: CP Violation*, *JHEP* **1107** (2011) 067, [[arXiv:1105.0376](#)].
- [17] N. Isgur and M. B. Wise, *Relationship Between Form-factors in Semileptonic \bar{B} and D Decays and Exclusive Rare \bar{B} Meson Decays*, *Phys.Rev.* **D42** (1990) 2388–2391.
- [18] J. Charles, A. Le Yaouanc, L. Oliver, O. Pene, and J. Raynal, *Heavy to light form-factors in the heavy mass to large energy limit of QCD*, *Phys.Rev.* **D60** (1999) 014001, [[hep-ph/9812358](#)].
- [19] B. Grinstein and D. Pirjol, *Symmetry breaking corrections to heavy meson form-factor relations*, *Phys.Lett.* **B533** (2002) 8–16, [[hep-ph/0201298](#)].
- [20] M. Beneke, G. Buchalla, M. Neubert, and C. Sachrajda, *Penguins with Charm and Quark-Hadron Duality*, *Eur.Phys.J.* **C61** (2009) 439–449, [[arXiv:0902.4446](#)].
- [21] J. Lyon and R. Zwicky, *Resonances gone topsy turvy - the charm of QCD or new physics in $b \rightarrow s\ell^+\ell^-$?*, [[arXiv:1406.0566](#)].
- [22] F. Kruger and J. Matias, *Probing new physics via the transverse amplitudes of $B_0 \rightarrow K^{*0}(\rightarrow K^-\pi^+)\ell^+\ell^-$ at large recoil*, *Phys.Rev.* **D71** (2005) 094009, [[hep-ph/0502060](#)].

- [23] U. Egede, T. Hurth, J. Matias, M. Ramon, and W. Reece, *New observables in the decay mode $\bar{B}_d \rightarrow \bar{K}^{*0}l^+l^-$* , *JHEP* **0811** (2008) 032, [[arXiv:0807.2589](#)].
- [24] S. Descotes-Genon, T. Hurth, J. Matias, and J. Virto, *Optimizing the basis of $B \rightarrow K^*\ell^+\ell^-$ observables in the full kinematic range*, *JHEP* **1305** (2013) 137, [[arXiv:1303.5794](#)].
- [25] U. Egede, T. Hurth, J. Matias, M. Ramon, and W. Reece, *New physics reach of the decay mode $\bar{B} \rightarrow \bar{K}^{*0}\ell^+\ell^-$* , *JHEP* **1010** (2010) 056, [[arXiv:1005.0571](#)].
- [26] D. Becirevic and E. Schneider, *On transverse asymmetries in $B \rightarrow K^*l^+l^-$* , *Nucl.Phys.* **B854** (2012) 321–339, [[arXiv:1106.3283](#)].
- [27] J. Matias, F. Mescia, M. Ramon, and J. Virto, *Complete Anatomy of $\bar{B}_d \rightarrow \bar{K}^{*0}(\rightarrow K\pi)l^+l^-$ and its angular distribution*, *JHEP* **1204** (2012) 104, [[arXiv:1202.4266](#)].
- [28] D. Das and R. Sinha, *New Physics Effects and Hadronic Form Factor Uncertainties in $B \rightarrow K^*\ell^+\ell^-$* , *Phys.Rev.* **D86** (2012) 056006, [[arXiv:1205.1438](#)].
- [29] S. Descotes-Genon, J. Matias, M. Ramon, and J. Virto, *Implications from clean observables for the binned analysis of $B \rightarrow K^*\mu^+\mu^-$ at large recoil*, *JHEP* **1301** (2013) 048, [[arXiv:1207.2753](#)].
- [30] S. Descotes-Genon, J. Matias, and J. Virto, *Understanding the $B \rightarrow K^*\mu^+\mu^-$ Anomaly*, *Phys.Rev.* **D88** (2013), no. 7 074002, [[arXiv:1307.5683](#)].
- [31] W. Altmannshofer and D. M. Straub, *New physics in $B \rightarrow K^*\mu\mu?$* , *Eur. Phys. J.* **C73** (2013) 2646, [[arXiv:1308.1501](#)].
- [32] F. Beaujean, C. Bobeth, and D. van Dyk, *Comprehensive Bayesian analysis of rare (semi)leptonic and radiative B decays*, *Eur.Phys.J.* **C74** (2014), no. 6 2897, [[arXiv:1310.2478](#)].
- [33] T. Hurth and F. Mahmoudi, *On the LHCb anomaly in $B \rightarrow K^*\ell^+\ell^-$* , *JHEP* **1404** (2014) 097, [[arXiv:1312.5267](#)].
- [34] J. Matias and N. Serra, *Symmetry relations between angular observables in $B^0 \rightarrow K^*\mu^+\mu^-$ and the LHCb P'_5 anomaly*, *Phys.Rev.* **D90** (2014), no. 3 034002, [[arXiv:1402.6855](#)].
- [35] S. Descotes-Genon, L. Hofer, J. Matias, and J. Virto, *On the impact of power corrections in the prediction of $B \rightarrow K^*\mu^+\mu^-$ observables*, *JHEP* **1412** (2014) 125, [[arXiv:1407.8526](#)].
- [36] W. Altmannshofer and D. M. Straub, *New physics in $b \rightarrow s$ transitions after LHC run 1*, *Eur. Phys. J.* **C75** (2015), no. 8 382, [[arXiv:1411.3161](#)].
- [37] R. Mandal, R. Sinha, and D. Das, *Testing New Physics Effects in $B \rightarrow K^*\ell^+\ell^-$* , *Phys. Rev.* **D90** (2014), no. 9 096006, [[arXiv:1409.3088](#)].
- [38] W. Altmannshofer and D. M. Straub, *Implications of $b \rightarrow s$ measurements*, in *Proceedings, 50th Recontres de Moriond Electroweak interactions and unified theories*, pp. 333–338, 2015. [[arXiv:1503.06199](#)].
- [39] R. Mandal and R. Sinha, *Implications from $B \rightarrow K^*\ell^+\ell^-$ observables using 3fb^{-1} of LHCb data*, [[arXiv:1506.04535](#)].
- [40] **LHCb** Collaboration, R. Aaij et al., *Differential branching fraction and angular analysis of the decay $B^0 \rightarrow K^{*0}\mu^+\mu^-$* , *JHEP* **08** (2013) 131, [[arXiv:1304.6325](#)].
- [41] **LHCb** collaboration Collaboration, R. Aaij et al., *Measurement of Form-Factor-Independent Observables in the Decay $B^0 \rightarrow K^{*0}\mu^+\mu^-$* , *Phys.Rev.Lett.* **111** (2013), no. 19 191801, [[arXiv:1308.1707](#)].

- [42] **LHCb** Collaboration, *Angular analysis of the $B^0 \rightarrow K^{*0} \mu^+ \mu^-$ decay*, *LHCb-CONF-2015-002, CERN-LHCb-CONF-2015-002* (2015).
- [43] **LHCb** Collaboration, R. Aaij et al., *Angular analysis of the $B^0 \rightarrow K^{*0} \mu^+ \mu^-$ decay*, [arXiv:1512.04442](https://arxiv.org/abs/1512.04442).
- [44] M. Ciuchini, E. Franco, G. Martinelli, M. Pierini, and L. Silvestrini, *Charming penguins strike back*, *Phys.Lett.* **B515** (2001) 33–41, [[hep-ph/0104126](https://arxiv.org/abs/hep-ph/0104126)].
- [45] M. Ciuchini, E. Franco, G. Martinelli, M. Pierini, and L. Silvestrini, *Searching For New Physics With $B \rightarrow K \pi$ Decays*, *Phys.Lett.* **B674** (2009) 197–203, [[arXiv:0811.0341](https://arxiv.org/abs/0811.0341)].
- [46] M. Duraisamy and A. L. Kagan, *Power corrections in $e^+ e^- \rightarrow \pi^+ \pi^-$, $K^+ K^-$ and $B \rightarrow K \pi$, $\pi \pi$* , *Eur.Phys.J.* **C70** (2010) 921–925, [[arXiv:0812.3162](https://arxiv.org/abs/0812.3162)].
- [47] A. Khodjamirian, T. Mannel, A. Pivovarov, and Y.-M. Wang, *Charm-loop effect in $B \rightarrow K^{(*)} \ell^+ \ell^-$ and $B \rightarrow K^* \gamma$* , *JHEP* **1009** (2010) 089, [[arXiv:1006.4945](https://arxiv.org/abs/1006.4945)].
- [48] S. Jäger and J. Martin Camalich, *On $B \rightarrow V \ell \ell$ at small dilepton invariant mass, power corrections, and new physics*, *JHEP* **1305** (2013) 043, [[arXiv:1212.2263](https://arxiv.org/abs/1212.2263)].
- [49] S. Jäger and J. Martin Camalich, *Reassessing the discovery potential of the $B \rightarrow K^* \ell^+ \ell^-$ decays in the large-recoil region: SM challenges and BSM opportunities*, [arXiv:1412.3183](https://arxiv.org/abs/1412.3183).
- [50] K. G. Chetyrkin, M. Misiak, and M. Munz, *$|\Delta F| = 1$ nonleptonic effective Hamiltonian in a simpler scheme*, *Nucl.Phys.* **B520** (1998) 279–297, [[hep-ph/9711280](https://arxiv.org/abs/hep-ph/9711280)].
- [51] P. Ball and R. Zwicky, *New results on $B \rightarrow \pi, K, \eta$ decay form factors from light-cone sum rules*, *Phys.Rev.* **D71** (2005) 014015, [[hep-ph/0406232](https://arxiv.org/abs/hep-ph/0406232)].
- [52] P. Ball and R. Zwicky, *$B_{d,s} \rightarrow \rho, \omega, K^*, \phi$ decay form-factors from light-cone sum rules revisited*, *Phys.Rev.* **D71** (2005) 014029, [[hep-ph/0412079](https://arxiv.org/abs/hep-ph/0412079)].
- [53] A. Khodjamirian, T. Mannel, and N. Offen, *Form-factors from light-cone sum rules with B -meson distribution amplitudes*, *Phys.Rev.* **D75** (2007) 054013, [[hep-ph/0611193](https://arxiv.org/abs/hep-ph/0611193)].
- [54] A. Bharucha, D. M. Straub, and R. Zwicky, *$B \rightarrow V \ell^+ \ell^-$ in the Standard Model from Light-Cone Sum Rules*, [arXiv:1503.05534](https://arxiv.org/abs/1503.05534).
- [55] R. Horgan, Z. Liu, S. Meinel, and M. Wingate, *Rare B decays using lattice QCD form factors*, *PoS LATTICE2014* (2015) 372, [[arXiv:1501.00367](https://arxiv.org/abs/1501.00367)].
- [56] S. W. Bosch and G. Buchalla, *The Radiative decays $B \rightarrow V$ gamma at next-to-leading order in QCD*, *Nucl. Phys.* **B621** (2002) 459–478, [[hep-ph/0106081](https://arxiv.org/abs/hep-ph/0106081)].
- [57] “Hepfit, a tool to combine indirect and direct constraints on high energy physics.” <http://hepfit.roma1.infn.it/>.
- [58] A. Caldwell, D. Kollar, and K. Kroninger, *BAT: The Bayesian Analysis Toolkit*, *Comput. Phys. Commun.* **180** (2009) 2197–2209, [[arXiv:0808.2552](https://arxiv.org/abs/0808.2552)].
- [59] **LHCb** Collaboration, R. Aaij et al., *Measurement of the $B^0 \rightarrow K^{*0} e^+ e^-$ branching fraction at low dilepton mass*, *JHEP* **05** (2013) 159, [[arXiv:1304.3035](https://arxiv.org/abs/1304.3035)].
- [60] **LHCb** Collaboration, R. Aaij et al., *Angular analysis of the $B^0 \rightarrow K^{*0} e^+ e^-$ decay in the low- q^2 region*, *JHEP* **04** (2015) 064, [[arXiv:1501.03038](https://arxiv.org/abs/1501.03038)].
- [61] C. Bobeth, M. Misiak, and J. Urban, *Photonic penguins at two loops and $m(t)$ dependence of $BR[B \rightarrow X(s) \ell^+ \ell^-]$* , *Nucl.Phys.* **B574** (2000) 291–330, [[hep-ph/9910220](https://arxiv.org/abs/hep-ph/9910220)].

- [62] C. Bobeth, P. Gambino, M. Gorbahn, and U. Haisch, *Complete NNLO QCD analysis of anti- $B \rightarrow X(s) l^+ l^-$ and higher order electroweak effects*, *JHEP* **0404** (2004) 071, [[hep-ph/0312090](#)].
- [63] P. Gambino, M. Gorbahn, and U. Haisch, *Anomalous dimension matrix for radiative and rare semileptonic B decays up to three loops*, *Nucl.Phys.* **B673** (2003) 238–262, [[hep-ph/0306079](#)].
- [64] M. Misiak and M. Steinhauser, *Three loop matching of the dipole operators for $b \rightarrow s$ gamma and $b \rightarrow s g$* , *Nucl.Phys.* **B683** (2004) 277–305, [[hep-ph/0401041](#)].
- [65] **Particle Data Group** Collaboration, K. A. Olive et al., *Review of Particle Physics*, *Chin. Phys.* **C38** (2014) 090001.
- [66] **ATLAS, CDF, CMS, D0** Collaboration, *First combination of Tevatron and LHC measurements of the top-quark mass*, [arXiv:1403.4427](#).
- [67] V. Lubicz. private communication.
- [68] F. Sanfilippo, *Quark Masses from Lattice QCD*, *PoS LATTICE2014* (2015) 014, [[arXiv:1505.02794](#)].
- [69] S. Aoki et al., *Review of lattice results concerning low-energy particle physics*, *Eur. Phys. J.* **C74** (2014) 2890, [[arXiv:1310.8555](#)].
- [70] P. Ball and V. M. Braun, *Exclusive semileptonic and rare B meson decays in QCD*, *Phys. Rev.* **D58** (1998) 094016, [[hep-ph/9805422](#)].
- [71] **UTfit** Collaboration, M. Bona et al., *The Unitarity Triangle Fit in the Standard Model and Hadronic Parameters from Lattice QCD: A Reappraisal after the Measurements of Delta $m(s)$ and $BR(B \rightarrow \tau \nu(\tau))$* , *JHEP* **10** (2006) 081, [[hep-ph/0606167](#)].
- [72] **UTfit** Collaboration. online update at <http://utfit.org>.
- [73] **CLEO** Collaboration, T. E. Coan et al., *Study of exclusive radiative B meson decays*, *Phys. Rev. Lett.* **84** (2000) 5283–5287, [[hep-ex/9912057](#)].
- [74] **Belle** Collaboration, M. Nakao et al., *Measurement of the $B \rightarrow K^* \gamma$ branching fractions and asymmetries*, *Phys. Rev.* **D69** (2004) 112001, [[hep-ex/0402042](#)].
- [75] **BaBar** Collaboration, B. Aubert et al., *Measurement of Branching Fractions and CP and Isospin Asymmetries in $B \rightarrow K^*(892)\gamma$ Decays*, *Phys. Rev. Lett.* **103** (2009) 211802, [[arXiv:0906.2177](#)].
- [76] T. Ando, *Predictive bayesian model selection*, *American Journal of Mathematical and Management Sciences* **31** (2011), no. 1-2 13–38. <http://dx.doi.org/10.1080/01966324.2011.10737798>.
- [77] A. Gelman, J. B. Carlin, H. S. Stern, and D. B. Rubin, *Bayesian data analysis*. Texts in Statistical Science Series. Chapman & Hall/CRC, Boca Raton, FL, second ed., 2004.
- [78] **LHCb** Collaboration, R. Aaij et al., *Test of lepton universality using $B^+ \rightarrow K^+ \ell^+ \ell^-$ decays*, *Phys. Rev. Lett.* **113** (2014) 151601, [[arXiv:1406.6482](#)].
- [79] S. Descotes-Genon, L. Hofer, J. Matias, and J. Virto, *Global analysis of $b \rightarrow s \ell \ell$ anomalies*, [arXiv:1510.04239](#).
- [80] R. R. Horgan, Z. Liu, S. Meinel, and M. Wingate, *Lattice QCD calculation of form factors describing the rare decays $B \rightarrow K^* \ell^+ \ell^-$ and $B_s \rightarrow \phi \ell^+ \ell^-$* , *Phys.Rev.* **D89** (2014) 094501, [[arXiv:1310.3722](#)].

- [81] M. Misiak, *The $b \rightarrow se^+e^-$ and $b \rightarrow s\gamma$ decays with next-to-leading logarithmic QCD corrections*, *Nucl. Phys.* **B393** (1993) 23–45. [Erratum: *Nucl. Phys.*B439,461(1995)].
- [82] A. J. Buras and M. Munz, *Effective Hamiltonian for $B \rightarrow X(s) e^+ e^-$ beyond leading logarithms in the NDR and HV schemes*, *Phys.Rev.* **D52** (1995) 186–195, [[hep-ph/9501281](#)].